1993

Development of Algorithms and Programs for the Ray Radiotomography of the Ionosphere.

Final (12-month) report (EOARD Contract SPC 93-4047)

CONTENT

Principal investigator

Professor V.Kunitsyn

1. Introduction.

We shall consider the potentials of radiotomography (RT) using phase and phase-difference measurements. Task of the ray RT of large-scale structures are usually formulated as follows: making use of measurements of linear integrals for series of rays intersecting a certain area, it is necessary to reconstruct the structure of this area. Since the dimensions of large inhomogeneities of natural (such as an ionospheric trough) or artificial origin (traces of spacecraft, technological releases etc.) are of hundreds and thousands kilometers, the diffraction effects in the case of VHF/UHF probing can be neglected [1,2].

It seems to be not possible even to name the kinds and types of emissions and waves for which attempts, at least theoretically, have not been made to apply tomographic methods. It makes no sense here to list all of the variants of tomographic approaches, but perhaps we should briefly characterize the approaches in the closest fields of tomography of geophysical structures. The methods and equipment for seismic tomography, where the distribution of the seismic "slowness", which is a value which is the inverse of the wave velocity, is reconstructed from measurements of the propagation time of seismic waves, have now been developed rather well. There is a very large number of works on seismic tomography; we will only cite certain surveys [3-5]. Many solution methods and algorithms have been proposed in the field of seismic tomography which are also suitable for other types of waves. Tomographic studies of other "spheres" of the Earth are also carried out. Acoustic tomography of the ocean, where the propagation time of acoustic waves is also measured, is now being developed actively [6,7]. Works on radio and optical

tomography of the atmosphere have appeared [8,9].

Proposals on variants of RT of the ionosphere have also been offered. A tomographic methods for determining the local attenuation factor as a function of geographic coordinates using data on the integral attenuation factors on paths covering a given region with a sufficiently dense network is discussed in [10,11]. Emitters and receivers far from the region to be reconstructed provide straight propagation paths. It was suggested to use the Radon transformation, which is practically unfeasible due to a small number of rays, besides, the question of the dependence of the attenuation factor on height remains to be settled. A variant of RT using a satellite, where reconstruction of the electron concentration distribution from the TEC on a series of rays was proposed, was examined in [12,13]. The data acquisition scheme is shown in Fig.0, where three receiving stations are located on the plane of passage of the satellite and the rays are assumed to be linear. The schemes for tomography according to linear integrals for various types of waves are indistiguishable from one another. The approach according to the ray integral electron concentration examined in [12,13] is identical, for example, to seismic interstitial tomography [14], where the sources of seismic waves are placed in bore holes, while the receiver is moved along the surface. More recently, methods of the RT of the ionosphere using the TEC have been developed by many investigators [15-23].

From our point of view such a generalization of tomography using linear integrals or TEC is enough obvious. The problem is how to determine this absolute phase or the linear integral. Many investigators attempted to answer this question and discussed difficulties. Here a nontrivial point is that when determining the absolute phase proportianal to TEC, the problem of determining the

"initial phase" arises and one can make a significant error and be off by a constant, which would lead to inconsistent tomographic data and render the reconstruction unfeasible. Unfortunately the authors of earlier publications on the ionosphere tomography merely presented this common and evident idea and failed to show the possibility of the reconstruction in the presence of typical errors, that is they did not model the influence of errors at the initial stages on the reconstruction results. The above comments should not be understood as diminishing the significance of the earlier studies on ionospheric RT, of special importance are studies on limitations of ionospheric RT and resolution limits imposed by geometrical and sampling limitations in ionospheric RT [15,16]. However, the authors of the earlier works restricted themselves to simulating the possibility of reconstructing the function using linear integrals, which was of little use since such simulation with the term substitution ("group delays" → TEC, "seismic slowness distribution" → "electron concentration distribution" and so on) has been made in numerous earlier works on seismic and other kinds of tomography. In contrast to seismics, however, where a linear integral (a group delay) is measured directly, for the ionosphere there are techniques for only approximate determination of linear integrals. Here a specific error appears - an error by a constant, which is essential for tomography. In direct measurements of linear integrals this error has, as a rule, a noise-like nature, which does not seriously affect the results. As discussed earlier [1,2,24] and will be shown below in section 4, the phase RT leads to poor results in the case of typical errors in determining the absolute phase or TEC. Therefore, some years ago [2,24] we proposed the phase-difference RT of the ionosphere.

The theoretical foundation of the ray RT is the well-known relations [25,1] for phase of radiowaves in the geometrical optics approximation. The following equality determines linear integrals from the electron concentration distribution N:

$$\lambda r_e \int N \, d\sigma = \phi, \qquad (1)$$

where λ is length of probing wave, r_e is the classical electron radius, $\omega=kc$, k is the wave number in the free space, c is the velocity of light, $\int d\sigma$ is the symbol of integrating by the ray. Here the linear integrals are the phase difference $\phi = \Phi_0 - \Phi$ of the field being measured ($E=A\exp(i\Phi)$) and the probing wave field ($E_0=A_0\exp(i\Phi_0)$). Measurements of ϕ are realized by receiving signals at two coherent frequencies from navigation satellites.

We introduce a series of parameters characterizing the geometry of the recording scheme in polar coordinates (r, α). In Fig.0 (r_0, α_0) - are the coordinates of the satelliite, (R, α_i) - are the coordinates of one of the receivers located on the surface of the earth (r=R); β is the elevation of the satellite; $\phi = (\beta-\pi/2)$ is the angle to the satellite measured from vertical; 0 is the center of the earth; axis 0-0' is axis of the polar coordinate system. On the basis of simple geometrical relations for any point in the ionosphere with coordinates (r, α) located at the distance of l from the receiver the foollowing equations are satisfied:

$$\frac{l}{\sin(\alpha_i-\alpha)} = \frac{r}{\sin(\pi/2+\beta)} = \frac{R}{\sin(\pi-(\pi/2+\beta)-(\alpha_i-\alpha))}.$$

From this, we obtain an equation for $r(\alpha)$ of the straight (β=const) ray

$$r(\alpha) = (R\cos\beta)/(\cos(\beta + \alpha_i - \alpha)) \qquad (2)$$

and the relation which is inverse of it

$$\alpha(r) = \alpha_i + \beta - \arccos\left(\frac{R}{r}\cos\beta\right). \qquad (3)$$

The relation between β and α, r follows from (2):

$$\operatorname{tg}\beta = (\cos(\alpha_i-\alpha) - R/r)/(\sin(\alpha_i-\alpha)). \qquad (4)$$

Using (3), we obtain a formula for an element of the ray of length $d\sigma$

$$d\sigma^2 = [1 + r^2(\frac{d\alpha}{dr})^2]\, dr^2 = \frac{r^2}{r^2 - R^2\cos^2\beta}\, dr^2. \qquad (5)$$

Then, the relation for the measured linear integral (1) with respect to the electron concentration will have the form

$$\phi = \lambda r_e \int N(r,\alpha)\, d\sigma = \lambda r_e \int \frac{N(r,\alpha)\, r\, dr}{\sqrt{r^2 - R^2\sin^2\psi}}. \qquad (6)$$

In the place of the polar coordinates (r, α), hereafter it is convenient to use the orthogonal system (h, τ): h=(r-R) is the height above the earth's surface and $\tau = \alpha R$ is the "transverse" (horizontal) distance along the earth's surface in the plane of passage of the satellite. Here, ray equation (2) will no longer be a straight line

$$h(\tau) = R\left[\frac{\cos\beta}{\cos(\beta+(\tau_i-\tau)/R)} - 1\right]. \qquad (7)$$

Here, $(\tau_i, h=0)$ are the coordinates of the receivers. The relation which is the inverse of (7) is similar to (3).

$$\tau - \tau_i = R\left[\beta - \arccos\left(\frac{R}{R+h}\cos\beta\right)\right]. \qquad (8)$$

In this case, subject to (5), the linear integrals of type (1) have the form

$$\int_0^{h_0} \frac{F(h,\tau)(R+h)dh}{\sqrt{R^2\sin^2\beta + 2Rh + h^2}} = I(\beta,\tau_i). \qquad (9)$$

Integration with respect to the ray connecting receiver i ($\tau_i=\alpha_i R$) to the satellite is replaced according to (5) by integration with respect to the height from surface of the earth to the height of the satellite h_0. The elevation β is determined (4) by position of the satellite (h_0,τ_0). The linear integral $I(\beta,\tau_i)$ is dependent on the coordinate of the receiver τ_i and the elevation of the satellite β. The linear integral is the complete phase ϕ (1); here, the reconstructed function F will be proportional to N. Since there cannot be a large number of receivers and the range of angles β is limited, it is inadvisable to examine methods for analytical inversion of such linear integrals and methods for integral transformations. In given case small-aspect tomography is intended from the start to solve the problem in discrete form and to use algebraic reconstruction algorithms or methods for expansion into finite series.

At first we will examine the possibility for replacing ray (7) by straight line. The ray became curved after the switch to the new coordinates (h,τ) convenient for solution of the of the discrete problem. The straight ray connecting the receiver ($h_i=0$, $\tau_i=0$) and the satellite (h_0, τ_0) is defined by the function $h'(\tau)= = \tau \operatorname{ctg} \phi_0$, which differs from the dependence

$$h(\tau) = R \left[\sin\phi/\sin(\phi-\tau/R) - 1 \right],$$

where $h(\tau_0) = h'(\tau_0) = h_0$. Expanding in powers of the small component $\tau/R \ll \phi$, we find that the height difference Δh between the two trajectories is expressed by the formula

$$\Delta h = h'(\tau)-h(\tau) \approx \frac{\tau_0}{R}(-\frac{1}{2} + \operatorname{ctg} \phi_0^2)\tau - \frac{\tau^2}{R}(-\frac{1}{2} + \operatorname{ctg}^2\phi_0) + O(\frac{\tau^3}{R^2}).$$

In the middle $\tau=\tau_0/2$ of the trajectory where $\phi_0= \pi/4$, $h_0=1000$ km, $\Delta h \approx 60$ km. From this, the division of the ionosphere into vertical increments should significantly exceed Δh if the curvature of the ray in coordinates (h,τ) is considered or, otherwise, if "curvature" of the polar coordinates in the region of reconstruction using a straight ray is not considered. The total phase will be even more sensitive to a failure to consider the curvature of the ray if we attempt to reconstruct N from the complete phase, since the lengths of the curved and straight rays will differ significantly. In short, consideration of the curvature of the polar coordinates in the region of reconstruction or of the curvature of the ray in coordinates (h,τ) in ray ionospheric RT of global structures is necessary, which is, unfortunately, not taken into account in a number of works [13,17,18].

1. The solution of the direct problem of radio wave propagation for the Ionospheric Tomography.

The purpose of this section is to describe the technique and program for solving the direct problem of ionosphere radio probing, i.e. the problem of obtaining the phase and the phase difference from the date on the electron density distribution. In view of calculation the direct problem solution amounts to calculatiry the integral (9), i.e. the phase or the difference of such integrals (the phase difference) for a small variation of the satellite position angle β. For the computer modeling of RT problems it is necessary to calculate a series of such integrals for arbitrary positions of the receivers and the satellite, therefore we accomplished the program for calculating the phase and the phase difference for arbitrary positions of the receivers and the satellite.

Since the integrand has no peculiarities, the calculation can be performed using the rectangle technique or the Simpson method. Let us evaluate the necessary step of numerical integration and the accuracies obtained in this way. It is well known that errors of numerical integration by the rectangle method ε_r and the Simpson method ε_s are equal to:

$$\varepsilon_r = \frac{h_0^3}{12}\frac{F^{(2)}}{m^2}, \qquad \varepsilon_s = \frac{h_0^5}{2880}\frac{F^{(4)}}{m^4}, \qquad (10)$$

where h_0 is the integration interval length (the satellite height), m is the number of the integral discretization elements. Integration errors made using the rectangle and Simpson methods are proportional to the values of the second and fourth derivatives, respectively, of the integrand at a certain point within the integration interval. For an approximate estimation of

errors it is sufficient to evaluate the second and fourth derivatives as a result of dividing a characteristic value of the function F by the square or the fourth power "a", respectively, of the structural irregularities of F. Limitations associated with diffraction effects as well as those of the linear tomography problem make it impossible to reconstruct details smaller than 10-20 km using the method of ray RT [1,2], therefore a $\geqslant$ 10-20 км. The value of m is equal to the result of dividing h_0 by the integration step Δh. Hense the estimations of absolute and relative errors are:

$$\varepsilon_r \leqslant \frac{h_0 F}{12} (\Delta h/a)^2, \qquad \varepsilon_s \leqslant \frac{h_0 F}{2880} (\Delta h/a)^5. \tag{11}$$

$$\frac{\varepsilon_r}{I} \simeq \frac{\varepsilon_r}{h_0 F} \leqslant (\Delta h/a)^2/12, \qquad \frac{\varepsilon_s}{I} \simeq \frac{\varepsilon_s}{h_0 F} \leqslant (\Delta h/a)^5/2880,$$

When the integration step Δh=0.5 км and a=20km the relative error of the rectangle method is $0.5*10^{-4}$ (for the Simpson method it is smaller than 10^{-11}) which is quite satisfactory for RT applications.

For further computer modeling of the RT problems it is necessary to use a set of appropriate electron density distributions models of the ionoshere. Naturally, it is impossible to make up a complete set of all the cinceivable ionospheric conditions, and this study was not aimed to do so. For our purpose - to illustrate the applications, which includes the main structural features (a trough, localized natural and man-made irregularities and groups of irregularities). Horewer, the presented package of programs makes it easy to design many other structural types and to extend this "ZOO" as far as possible using the available "details". In what follows the available "details"

and the models used are described.

Description of the set of the models used for reconstruction.

The "parabola" (with a discontinuity of the first derivative) and the "cosine square" (with no discontinuity of the first derivative), a "gaussian" are used as the functions to describe localized irregularities. Cross-sections of the constant value for such irregularities may be arbitrary oriented ellipses.

No.1. A simple model of the ionosphere with a trough and a positive irregularity at the left edge of the trough is represented in Fig.1 in isolines in the $10^6 cm^{-3}$ units.

No.2. A model of the ionosphere with a trough and three inhomogeneities (all of them being of the "cosine-square" type, the positive one is at the left edge of the trough, the other positive one is also at the height of the maximum at the opposite edge of the trough, the negative irregularitity is located higher (h=500km, τ = 500km)) representated in Fig.2 in isolines in the $10^6 cm^{-3}$ units.

No.3. A model of a homogeneous smooth ionosphere with a chain of irregularities in the region of the main maximum. The model is represented in Fig.3 in isolines in the $10^6 cm^{-3}$ units.

No.4. The model of the heated ionospheric lens [26]. The maximum of ΔN is equal $\Delta N=10^4 cm^{-3}$. $N(h,\tau)=N_0(h_0/G(h))^2(1-\tau^2/G^2\theta_0^2)$, $\tau \leqslant G(h)\theta_0$, $G(h)=(h^2+\gamma(h-h_0^2))^{1/2}$, h_0=100 km, γ=3, θ_0=0,15 (Fig.4).

No.5. A model of a localized irregularity described by 3 "gaussians". The sizes of the disturbed region are 100 x 100 km.

No.6. A group of isolated irregularities (Fig.6) described by the "cosine square" functions.

No.7. A model (Fig.7) of a localized simple irregularity described by two "cosine square". The sizes of the disturbed region are 100 x 100 km, the hight is 200km.

Description of the program

for calculation the phase and the phase-difference for arbitrary positions of the receivers and the satellite.

System Requirements

- Computer:	IBM AT or compatible (with coprocessor)
- Operating System:	MS-DOS or PC-DOS version 3.0 and later
- Memory:	at least Extended memory 16 Mbytes (depends on geometry and type of approximation reconstructed function)
- Hard Disk Space:	16 Mbytes
- Software:	compiler 1.4e and linker 2.2d NDP-FORTRAN-386(c) MicroWay or later

1. Program <integr.for>

This program solves direct problem, namely, determines the model structure and calculates the phases or TEC for phase RT or doppler for phase-difference RT on the model structure.

Input parameters and files:

Answer=1 - Phase RT: Tec_ph=1 --> calculation of TEC
Tec_ph=2 --> calculation of Phase
Answer=2 - Phase-difference RT
Answer, Tec_ph are introduced from the screen
file <name_F.int> - names of output files for integrals for each receiver
NREC - number of receivers
NRAY - max number of rays
RAY - array of rays for each receiver
NF - number of discrets on the horizontal grid
NR - number of discrets on the vertical grid
NirMAX - max number of local irregularities for model
FP - array of receivers's polar angles in degrees
(FP(1)=0. -> for the first receiver)
RZ - Earth's radius in km

RO - satellite orbit in polar coordinate system in km
HFIST,HFIN - initial and final altitude of reconstructed
structure in km
F1 - horizontal distance to the left from first receiver
in km (F1<0)
F2 - horizontal distance to the right from last receiver
in km (F2>0)
Dconst - the value for determination of doppler (shift of rays)
NJ - number of discrets on the one ray for calculation
of integrals
RMAX - altitude of max electron density in km
The model structure is determined by function <FMODEL> which
uses functions <FUNC1>, <FUNC2>, <HOMPAR> or <HOMCOS> and input
file <F_mod>.
Input file <F_mod> contains parameters of model, for example:

```
<< 'number of irregularities and Zmax - max value of parabol'
   1 1.
   'local irregularities: Hirreg, Tirreg, A, B, Z'
   350. 36. 100. 100. 0.08
   'trough --> TGR1, TGR2 in km'
   -20. 640. >>
```

line 2 in file: 1 1.
Nirreg (number of irregularities)=1
Zmax=1.
line 4 in file: 350. 36. 100. 100. 0.08 -
Hir (altitude of irregularity in km)=350.
Tir (horizontal coordinate of irregularity in km) =36.
Air=100.- vertical size of irregularity
Bir=100.- horizontal size of irregularity
Zmax=0.08 - max value of irregularity
line 6 in file
-20. 640.
TGR1=-20., TGR2=640 - horizontal coordinates of trough in km

RMAX, RM, B1, B2, ZSM - parameters for function <FUNC1>
(model on h)
DEPTH, CONS1, CONS2 - parameters for function <FUNC2> (trough):
DEPTH - depth of trough
CONS1,CONS2- the egdes of trough

<HOMPAR> - approximation of local irregularity by parabol
<HOMCOS> - approximation of local irregularity by $\cos^2$

The combinations of <FUNC1>,<FUNC2>,<HOMPAR>,<HOMCOS> make it possible to obtaine different model structures.
Subroutine <DEFPSI> determinates the angles of rays on the satellite's coordinates
Subroutine <DEFINT> calculates either Phase or TEC or Doppler and uses subroutine <INTERG>.
Subroutine <INTERG> calculates integral only one ray on the model.

Output files:
MOD.GRD - file of model structure
Files <Fint> - arrays of either Phases or TEC or Doppler

Execution
f77 integr.for

RUN
integr.exp

2. Design of the different versions of the RT operators (matrices).

We shall consider the problems of the design of the different versions of the RT operators (matrices), beginning with discretization procedure for equations (1). We perform digitization of the linear integrals $I(\beta,\tau_i)$ (9) according to the position of the satellite, which is dependent on the coordinates τ_{0j} or the angle $\alpha_{0j}= \tau_{0j}/R$. The set of coordinates of the satellite τ_{0j} is recalculated according to (4) into a series of elevation β_{ij} of the satellite from receiver i:

$$\operatorname{tg}\beta_{ij} = \frac{(R + h_0)\cos(\alpha_i - \alpha_{0j}) - R}{(R + h_0)\sin(\alpha_i - \alpha_{0j})}. \qquad (12)$$

The sets of elevation of all receivers define a series of discrete values of the linear integrals $I_{ij} \equiv I(\beta_{ij}, \tau_i)$. The simplest method for digitization of the sought function $F(h,\tau)$ in a fixed rectangular $(m_0 \times n_0)$ grid is to replace it by a piecewise-constant approximation, or to represent F by a system of $(m_0 \times n_0)$ basis functions equal to unity in certain rectangle and zero in all others. The rectangular reconstruction region is divided into m_0 heights $(m \leqslant m_0)$ and n_0 horizontal samples $(1 \leqslant n \leqslant n_0)$. Let the value of the function $F(h,\tau)$ in a fixed $(m \times n)$ rectangle be F_{mn}. The point in the rectangles at which the samples of $F(h,\tau)$ are selected is not especially important; this may be at the middle of the rectangles or nodes of the grid.

The problem of tomographic reconstruction according to linear integrals is to determine the set of discrete samples $\{F_{mn}\}$ in the known grid according to the set $\{I_{ij}\}$. Designating the length of ray (i,j) in cell (m,n) as $L_{i,j}^{m,n}$, we obtain the system of linear

equations

$$L^{m,n}_{i,j} F_{m,n} = I_{i,j} \quad \text{or} \quad L^{M}_{J} F_{M} = I_{J} . \tag{13}$$

Here, "renumbering" of the ray $(i,j) \rightarrow J$ and the sells of the ionosphere $(m,n) \rightarrow M$ is performed in the second equation. The repeating indices are understood as summation. The number of rays is determined by the parameters of the recording system. The coefficients L_{JM} are calculated according to the given rays and cells into which the ionosphere is divided. System (13) may be either overdetermined or sub-definite.

Thus if there is a possibility to determine the linear integrals (1), the problems of the ray RT are reduced with the help of discretization procedure to solving systems of linear equations. But the problem of ionospheric RT according to phase-difference or Doppler measurements cannot be solved by such scheme with a piecewise-constant approximation. The fact is that the data here will be derivatives of linear integrals of type (9): $D = dI/d\alpha_0$, or finite-difference ratios of the increment ΔI of the linear integrals to the increment $\Delta\alpha_0$ of the satellite coordinate. The Doppler frequency $\Omega = d\phi/dt$ measured in the experiment is determined by the phase derivative (1). The relation between the angle α_0 of a satellite moving uniformly along a circular orbit with velocity v_0 and the time $\alpha_0 = v_0 t/(R+h_0)$ makes it possible to express the Doppler frequency Ω by means of the derivative with respect to the angle of the satellite

$$\Omega = \frac{v_0}{R+h_0} \frac{d\phi}{d\alpha_0},$$

from which these phase-difference tomography data are proportional to $\Delta I/\Delta\alpha_0$. The derivatives of the linear integrals in a

piecewise-constant approximation of the sought function F will be discontinuous. This is because each linear integral is the sum of integrals over the set of cells. As the elevation of the satellite changes, the ray encounters a new cell; the integral with respect to unity of this cell is a continuous function of the angle of the satellite α_0, but the derivative of the linear integral with respect to α_0 will contain a discontinuity when the ray contacts the corner of each cell. Therefore, the piecewise-constant representation of the function to be reconstructed does not make it possible to analyze the phase-difference problem.

Phase-difference measurements require higher-order interpolation than the piecewise-constant representation of the function to be recorded. Correspondingly, the matrix L_{JM} for transition from the function to be reconstructed to linear integrals should be calculated differently so as to ensure continuity of linear integrals with respect to the coordinate of the satellite α_0 (or elevation β). If the matrix of the direct problem L_{JM}: $F_M \to I_J$ is continuous with respect to the angle of the satellite α_0, then in place system (13) it is possible to obtain a system for phase-difference or Doppler data by differentiating (13) with respect to the angle α_0:

$$A_{JM}F_M = D_J \,. \qquad (14)$$

Here, $D_J \equiv \Delta I_J/\Delta\alpha_0$ are Doppler data and $A_{JM} \equiv \Delta L_M/\Delta\alpha_0$ is finite -difference ratio (or derivative) of the matrix L_{MJ} to the increment of the angle. The Doppler data are determined not only by the change in the complete phase related to integral electron concentration along the ray, but also the local electron concentration N_s at the point of the satellite. The correction to the Doppler data is equal to the product of N_s times the velocity

component of the satellite directed along the ray - $\lambda r_e N_s \cos(\alpha_i + \beta - \alpha_0)$. This correction can be inserted into the iteration algorithm and the values of N_s at the boundary $h=h_0$ of the ionosphere obtained in the iteration process will constantly "correct" the measured Doppler frequency values [25]. The question of whether such a correction of the data should be made can be answered depending on whether we use direct measurements of the Doppler frequency or the phase difference derived from phase measurements. In the former case such a correction should be made, in the latter - not. Here such a correction shall not be performed; horewer, it would not be difficult to introduce it when using direct doppler measurements.

In what follows we shall briefly describe the methods of constructing the operators that are smooth by the satellite angle; here are the examples of constructing the L_{JM} matrices of the transition from the reconstructed function to the linear integrals (matrices of projection operators) useful as for the phase-difference RT and also for the phase RT. In this section we consider examples of constructing smooth projection operators of the direct problem. One must construct such a L_{JM} matrix that would provide the smooth of linear integral over the satellite angle. In the beginning section we consider contribution on the basis of triangular elements, at the end of the section other possible variants be outlined. We will proceed to calculation of the matrix A_{JM} of the difference problem, which, as was already noted, should be determined from the increment of the matrix L_{JM} which is smooth with respect to the angle of the satellite. Smoothness of the matrix L_{JM} can be ensured by introducing finite triangular elements for representation of the function $F(h,\tau)$, i.e., when the sought function is replaced by a piecewise-planar

approximation. The smooth function $F(h,\tau)$ is replaced by a continuous polyhedral approximation surface, according to which the derivative with respect to the satellite angle of the linear integrals is already a continuous function. Triangular elements are obtained naturally from a grid of rectangles by dividing each of them in half diagonally. The function $F(h,\tau)$ within each triangular element is replaced by linear approximation

$$F(h,\tau) = a + b\tau + ch. \tag{15}$$

The values of the coefficients (a, b, c) in each finite element are determined from system of three equations for three boundary points. It is simple to immediately write expressions for the coefficients in a given finite element. These expressions differ slightly for triangular elements of two types: those occupying cells "below" or "above". We stipulate that cell (m,n)

$$(\tau_m, \tau_{m+1}) \times (h_n, h_{n+1}) = \Delta\tau \times \Delta h$$

is divided by a diagonal $(\tau_m, h_{n+1}) - (\tau_{m+1}, h_n)$ running downward and left-to-right, into two triangular elements: the "lower" and "upper" elements. Then, in the lower (m,n) element

$$F(h,\tau) = F_{m,n} + \frac{F_{m+1,n} - F_{m,n}}{\Delta\tau}(\tau-\tau_m) + \frac{F_{m,n+1} - F_{m,n}}{\Delta h}(h-h_n) \tag{16}$$

and in the upper (m,n) element

$$F(h,\tau) = F_{m+1,n+1} + \frac{F_{m+1,n+1} - F_{m,n+1}}{\Delta\tau}(\tau-\tau_{m+1}) +$$

$$+ \frac{F_{m+1,n+1} - F_{m+1,n}}{\Delta h}(h-h_{n+1}). \tag{17}$$

As before, to simplify the notation we will renumber the values of the samples below: $F_{m,n} \to F_M$, $(m+1,n) \to (M+1)$, $(m,n+1) \to (M+\Delta M)$,

$(m+1,n+1) \rightarrow (M+\Delta M+1)$, where ΔM is the number of cells horizontally in one row.

The linear integral I_J (9) is the sum of the integrals with respect to all finite elements which intersect ray J:

$$I_J = \sum_M \int \gamma(h)\, F(h,\tau)\, dh,$$

where $\gamma(h)=(R+h)[R^2\sin^2\beta+2Rh+h^2]^{-1/2}$, while $F(h,\tau)$ is represented in the form of piecewise-planar approximations (16),(17) in each finite element. The result of integration of such an approximation in lower element M

$$\int \gamma(h)F\, dh = J_0\, F_M + J_\tau(F_{M+1} - F_M) + J_h(F_{M+\Delta M} - F_M) \qquad (18)$$

and in upper triangular element M

$$\int \gamma(h)F\, dh = J'_0\, F_{M+\Delta M+1} + J'_\tau\, (F_{M+\Delta M+1} - F_{M+\Delta M}) + J'_h\, (F_{M+\Delta M+1} - F_{M+1}) \qquad (19)$$

Here, J_0, J_τ, J_h, J'_0, J'_τ, J'_h are the following integrals:

$$J_\tau = \frac{1}{\Delta\tau}\int_{h_n}^{h} \gamma(h)\,[\tau(h)-\tau_m]dh; \qquad J'_\tau = \frac{1}{\Delta\tau}\int_{h}^{h_{n+1}} \gamma(h)[\tau(h)-\tau_{m+1}]dh;$$

$$J_h = \frac{1}{\Delta h}\int_{h_n}^{h} \gamma(h)[h-h_n]dh; \qquad J'_h = \frac{1}{\Delta h}\int_{h}^{h_{n+1}} \gamma(h)[h-h_{n+1}]dh. \qquad (20)$$

Integration with respect to a lower finite element begins at the lower boundary of the cell $h=h_n$ and ends at height h, where the ray leaves the lower element. Integration with respect to the upper finite elements begins at this height and ends at the height of the upper boundary of the cell. We will recall that $\gamma(h)$ and all integrals with respect to cell M are functions of the

elevation β, α_0 or the number of the ray J.

After integration (18) with respect to ray J in the lower element M the value $(J_0 - J_\tau - J_h)$ is entered into the coefficient L_{JM}, since it is a coefficient for F_M. Correspondingly, J_τ is entered into $L_{J,M+1}$ and J_h into $L_{J,M+\Delta M}$. However, in integration with respect to one lower finite element M these coefficients L are still not completely determined. It is easy to understand that each sample F_m falls into three lower and three upper adjacent finite elements. Only after integration with respect to ray J in all finite elements is it possible to completely form the coefficient L_{JM} from six around F_m where the ray fell. Integration with respect to the upper finite element M with respect to ray J (19) makes the contribution $(J'_0 + J'_\tau + J'_h)$ to the coefficient $L_{J,M+\Delta M+1}$; the contribution $(-J'_\tau)$ to the coefficient $L_{J,M+\Delta M}$ and the contribution $(-J'_h)$ to the coefficient $L_{J,M+1}$. The integrals with respect to all rays of type (20) can be calculated by various numerical methods; in view of the smoothness of $\gamma(h)$ and the piecewise-planar approximation of F, it is sufficient to use the trapezoid or Simpson method. Here, in each integration step Δh it is necessary to verify that the ray does not exceed the limits of the finite element.

Performing numerical integration with respect to all rays, we obtain the matrix L_{JM}. The matrix L_{JM} is related to the set $\{\alpha_0\}$ of positions of the satellite and the corresponding series of rays. It is also possible to calculate the matrix L' for another set of close positions of the satellite with a fixed increment $\{\alpha_0+\Delta\alpha_0\}$. After this, we determine the matrix for phase-difference tomography problem $A_{JM} = (L'_{JM} - L_{JM})/\Delta\alpha_0$.

The projection operator or L_{JM} matrix can also be built on the basis of approximations of higher order than that of (15). For

example, one can use a two-dimensional approximation in the form of the product of linear functions or the product of cubic splines. Then the function $F(h,\tau)$ takes the form

$$F(h,\tau) = \sum_{m,n=0}^{3} a_{mn}\tau^m h^n \qquad (21)$$

Inside an arbitrary (m,n) rectangular, representing the function through the normalized coordinates $x=(\tau-\tau_m)/\Delta\tau$, $y=(h-h_n)/\Delta h$, we can obtain the following representation through the values of the function at the four angular points $(x,y)= \{(0,0); (0,1); (1,0); (1,1)\}$.

$$F(x,y) = F_{00}P_{00} + F^{x}_{00}P^{x}_{00} + F^{y}_{00}P^{y}_{00} + F^{xy}_{00}P^{xy}_{00} + F_{01}P_{01} + \ldots\ldots$$

Here the subscrips refer to the coordinates (x,y) of the angular points, F is the value of the function in corresponding point, F^x, F^y are the values of the function partial derivatives with respect to x,y, F^{xy}_{00} is the value of the function partial derivative of the second order with respect to x,y. The total sum (21) will contain 16 summands, $P^{\gamma}_{\alpha\beta}(x,y)$ are corresponding polynomials of the power not exceeding 3. We shall not write the mentioned polynimials completely, four examples will be suffice for illustration:

$$P_{00} = 4x^3y^3 - 6x^2y^3 - 6x^3y^2 + 9x^2y^2 + 2y^3 - 3y^2 + 2x^3 - 3x^2 + 1,$$

$$P^{x}_{00} = 2x^3y^3 - 4x^2y^3 - 3x^3y^2 + 6x^2y^2 + 2xy^3 - 3xy^2 + x^3 - 2x^2 + x,$$

$$P^{y}_{00} = 2x^3y^3 - 3x^2y^3 - 4x^3y^2 + 6x^2y^2 + 2x^3y - 3x^2y + y^3 - 2y^2 + y,$$

$$P^{xy}_{00} = x^3y^3 - 2x^2y^3 - 2x^3y^2 + 4x^2y^2 + x^3y - 2x^2y + xy^3 - 2x\,y^2 + xy.$$

.....

Then, integrating in each cell of the given polynomials we can produce the corresponding elements of the matrix, as in the case (16-20). Note, that now it is not only the values of the function F, but the values of the mensioned derivatives that are

unknown, i.e. such representation makes it possible to find the function and its first derivatives. The matrix for the product of linear approximations can be constructed in a similar, even simpler, way, this being in fact a particular case of that described above, where the summation in the formula is made up to 1 rather than up to 3.

Thus, the following operators (matrices) for solving the RT problems are described:

A - is built with the piece-constant approximation,

B - is built with the piece-planar approximation,

C - is built with the linear product approximation,

D - is built with the cubic spline product approximation.

Projection operators with approximations of higher orders allow a better approximation of the operator of the direct problem, i.e. they enable us to come closer to the true operator of the direct problem. Tables 1,2 shows examples of calculations of the direct problem for the model 2 and 5 with the help of different operators: A, B, C, D. Errors of the numerical simulation can appropriately be characterized by number δ, which shows the deviation of the function being reconstructed $\tilde{F}$ from the true function F: $\delta=\|F-\tilde{F}\|/\|F\|$. The norms of the spaces l^2 and l^∞ can be helpfully used ($\delta_2 \equiv \delta(l^2)$ and $\delta_\infty \equiv \delta(l^\infty)$). We use the data ($h_0$=1000km) from three receivers with coordinates τ_1= 0km, τ_2= 475 km, τ_3= 1435 km (for model 2, this geometry is similar to the geometry of Murmansk-Moscow RT experiments [1,2]) and τ_1=0, τ_2=240, τ_3=480 (model 5). From the results given in this tables one can clearly see the increased accuracy in solving the direct problem for operators with higher oders of approximation.

One can see that the transition to higher orders makes it possible to significantly improve the solution of the direct

problem. However, as the approximation order increases the matrix becomes more complicated and less rarefied, which can impair the solution of the inverse problem. One cannot say in advance which operator will be more preferable when solving the inverse problem, because at the beginning of the increase of the approximation order the function is approximated better but the matrix properties for solving the inverse problem become worse. Operators must be chosen by means of computer simulation to be illustrated in the next section.

Description of the program for calculation of the different versions of the RT matrices (operators).

2. Program <matric.for>

This program designs different versions of the operators (matrices) for phase RT or phase-difference RT.

Input parameters and files:

Parameters < Answer, NF, NR, NREC, NJ, RAY, HFIST, HFIN, F1, F2, RZ, RO, Dconst> are similar to same parameters of program <INTEGR.FOR>.

File <name_F.mat> contains names of output files

MOD.GRD - input file of model structure (program <INTEGR.FOR>)

APTYPE - type of approximation of reconstructed structure, it is introduced from the screen

Subroutine <DEFPSI> determinates the angles of rays on the satellite's coordinates.

Subroutine <DEFMAT> determinates the matric with corresponding approximation for one receiver

Output files:

Files <F_matr> - arrays of matric of corresponding approximation for each receiver

File <Fparam> - parameters of matrices for each receiver

Files <F_int> - results of multiplications of calculated matric and model structure

File <F_st> - array (LST) of number of all rays which cross the corresponding discret of model (SIRT algorithm)

Execution

f77 matric.for rayint.obj

RUN

matric.exp

3. The solution of the inverse problems of the phase and phase-difference RT.

It should be noted that the earlier authors solved problems of tomography using linear integrals, which amounted to solving systems of linear equations. In this respect, therefore, the problem of pure phase RT is entirely equivalent to the known problems on linear integrals. The peculiarity of ionospheric applications is revealed in the nature of possible errors by a conctant in determining the phase, which will be dealt with in the next section.

In this section varios methods of solving inverse problems of RT will be brifly described and analysed. The results obtained using various reconstruction methods and the sensitivities of these methods will be compared, which is of interest for ionospheric application. Solution of (13-14) in ray RT of the ionosphere is difficult in computational respects. When reconstructing global structures with dimensions of thousands kilometers and a sampling interval of tens kilometers, the matrices of such systems contain up to 10^6-10^7 elements, but are rather empty. There are a significant number of both direct and iterative methods for solving system of linear equations like (13-14). Nevertheless, intensive development of the theory and practical methods and algorithms for solution of these systems continues at present. There are a large number of diverse iterative methods for solving systems of linear equations. Many of them have been tested in ray RT problems. As was previously noted, tomographic methods have been developed most intensively in seismics, where various methods for solution of these system have been used. Here, we can cite algebraic reconstruction technique

(ART), including with relaxation and for systems of inequalities; simultaneous iteration reconstruction technique (SIRT); multiplicative algebraic reconstruction technique (MART); block-iterative algorithms, reconstruction on the basis of the Bayes approach, algorithms for regularization of the mean square error, algorithms for optimization of image entropy, etc. [36]. Good practical results have been obtained in seismic tomography using methods for minimization of the iterative corrections in various matrices with variants of weighted correction, ray weighing and inter-iteration smoothing [3]. Investigations have been made of the characteristics of the spectra of the matrices, the resolution of the reconstruction systems and the uniqueness of the reconstruction possible "at the limit", i.e., with an infinite increase in the number of measurements [5].

Since there are numerous methods of solving systems of linear equations, it appears to be impossible to apply all the known approaches within one study. It should be pointed out that the main results of the investigations perfomed are weakly dependent on the applied methods for solving systems of linear equations, here, therefore, we shall apply the most widely known methods: ART, SIRT, MART.

Before giving examples of RT-reconstructions, it is to be noted that in some cases there is a possibility of an accurate determination of the absolute phase. It is possible to determine the absolute phase at inhomogeneities when reconstructing the structure of sufficiently large localized artificial (releases, heating, etc.) or natural inhomogeneities of the ionosphere arising during the time between flights of the satellite. Such a formation being localized in space provide the possibility of solving the problem without additional a priori assumptions

concerning the inhomogeneity. By recording the data before and after the emergence of the disturbance and making subtraction of data, one can find the contribution of the localized inhomogeneity being reconstructed, if the ionosphere changes little between the flights.

Fig.8 shows the reconstruction of a heated ionospheric lens by phase RT after 20 ART iterations using the data from three receivers with coordinates τ_1=0 km, τ_2=45 km, τ_3=90 km, h_0 = 1000km. The height of the disturbed region varied from 80 to 220 km. The zeroth initial guess was given. The size of the division discrete was 10kmx10km. The reconstruction differs little from the model structure, the relative reconstruction errors being δ_2 = =0.07, δ_∞ =0.09. Also the simulation of the reconstructions of other localized formulations was carried out, thus showing the possibility to reconstruct structures of localized objects emerging between flights of the satellite using data on the absolute phase of this object.

In what follows the results of modeling the RT reconsctraction using different operators A,B,C,D are presented. Tables 2 and 3 show examples of calculations of the reconstruction results for the models 2, 5 and 7 with the help of different operators: A, B, C, D. Errors of the numerical simulation be characterized by number δ_2 and δ_∞ , which shows the ratio of the deviation of the function being reconstructed $\tilde{F}$ from the true function F. The reconstruction results must be compared in the norms approaching to the integral ones, i.e. the norms L^2 must be used instead of l^2 and L^∞ instead of l^∞ (the corresponding numbers Δ_2 and Δ_∞ instead of numbers δ_2 and δ_∞). In other words the functions must be compared using a much finer grid than that used for reconstruction. Otherwise, if the results are compared in

reconstruction points only, we may come to erroneous conclusions. We use the data from three receivers (similar to Murmansk-Moscow RT experiments [1,21]) with coordinates τ_1= 0 km, τ_2= 475 km, τ_3= 1435 km (for model 2), τ_1=0, τ_2=240, τ_3=480 (model 5) and τ_1=0, τ_2=250, τ_3=500, τ_4=750, τ_5=1000, (model 7). Figs.9 (A,B,C,D) show the RT reconstruction results for different approximations (A, B, C, D, respectively) of model 7. Figs.10 (B,C) show the RT reconstruction results for different approximations (B, C) of model 2. Fig.11 show the RT reconstruction result for approximation C of model 5 and fig.12 for approximation (D). From the reconstruction results and tables 2,3 one can see the increase in the accurasy of solving RT reconstruction problems for operators with higher orders of approximation.

The results of RT reconstruction also depend on the applied approach of the phase or phase-difference RT. If the conventional phase RT with the piece-constant (A) approximation is used, the phase-difference RT with matrices of the (B,C,D) type has, as a rule, an advantage connected with a more accurate representation of the direct problem operator. Figs.13 and 14 show the results of the RT reconstruction of model 2 using the methods of the phase (fig. 13) and phase-difference (fig. 14) RT. The homogenious ionosphere model (fig.15) was used as an initial approximation. Phase-difference RT allows a more precise isolation of local extrema and has a lower noise level. Note that, in general, the reconstruction results of rather large structures obtained using these methods providing there were no errors in determination of the initial phase are comparable. The presense of such an error, however, makes the phase RT method practically unsuitable, which will be shown by the results to be presented in the next section.

Let us analyse the results obtained by applying various

methods of solving systems of linear equations (SLE) for RT problems. It has already been mentioned that we shall restrict our consideration to the most widely used techniques, namely, the ART, SIRT and MART algirithms. Comparison of different algorithms of solving SLE must clearly be made for the same RT method. The results of comparing the SLE solution algorithms for the phase RT method will be illustrated by the reconstruction of model 6. Since reconstruction errors are determined both by the number of iterations and measurement errors, each algorithm should be characterized by a two-dimensional error "portrait" providing the dependence of a relative reconstruction error on the number of iterations and the relative error in the right-hand part of equation. Such an error portrait characterizes the convergence rate, the feasible minimum of the reconstruction error for different levels of data errors. The error portraits for the ART and MART algorithms are represented in figs. 16,17. One can see that for non-zero errors the algorithms begin diverging quite rapidly, the iteration process must, therefore, be stopped in the region of the reconstruction error minimum, whose position being determined by data errors. The SIRT algorithm (Fig.18) is significantly less sensitive to data errors owing to intermediate averaging of the results during the iteration process. The error level in the SIRT, however, is much higher ($\geqslant$43%) than those of the ART and MART algorithms. The numerical experiments performed with other models also showed that the SIRT algorithm is practically unsuitable due to the high level of reconstruction errors. This algorithm would be appropriate for use in the case of severe data errors ($\geqslant$5-10%). In this case, however, the SIRT algorithm would reconstruct a highly "averaged object" which bears little resemblance to the original structure. In general, the

reconstruction results obtained using the ART and MART algorithms are comparable: in some cases the ART has certain advantages, in other cases the MART is more appropriate.

Another advantage of phase-difference tomography over phase tomography should be noted, that is a higher sensitivity of the former. Doppler data are more sensitive to small inhomogeneities which have little affect on the phase. For example, when the ray scans the inhomogeneity ΔN of the size a, the phase changes by $\Delta\Phi \sim \lambda r_e \Delta Na$, here the relative change of the phase $\Delta\Phi/\Phi \sim \Delta Na/N_t \sim \sim \Delta Na/N_m L$, where N_t is the TEC along the ray, N_m is the value at the maximum electron concentration, L is the ray lenght characteristic. As a result, relative variations of the phase are proportional to the ratio of the TEC of the inhomogeneity to the TEC of the whole ionosphere. One should not expect the methods of solution of (13,14) to be more sensitive to changes of the right-hand part than a few percent. Therefore phase methods would not distinguish even sufficiently strong $\Delta N/N_m \sim$ 0.1 inhomogeneities with the size $a \leqslant L/10$ ($\leqslant$100km), since they produce only 1% of phase variations. It is not accidental, in our opinion, that in the reported reconstructions using the phase methods [18-20] details with dimensions of less than a few hungred kilometers are not revealed. This is not the case for phase-difference measurements. Here total Doppler variations are proportional to $d\phi/dt \sim \lambda r_e NL/(L/v_s)$, and Doppler variations at an inhomogeneity are $\sim \lambda r_e \Delta Na/(a/v_s)$. Then relative Doppler variations (phase differences) are proportional to the ratio of electron concentrations $\sim \Delta N/N_m$. Thus, the phase-difference methods allow the reconstruction of inhomogeneities of a few percent against the background regardless of the size of an inhomogeneity. This is fully supported by our experimental results [2,24,27-29].

To illustrate the estimation of the sensitivity of the methods, we shall consider the reconstruction results of model 3, with the chain of irregularities of the size a =100km and variations $\Delta N=0.025*10^{12}m^{-3}$ (the first two irregularities at the left) and $\Delta N=0.015*10^{12}m^{-3}$ (the next three irregularities), which amounts to 3-5% of the maximum $N_m=0.5*10^{12}m^{-3}$. Due to irregularities, variations of the total phase are a few parts of a percent and practically invisible in fig.19. In accordance with the above estimations, doppler variations are equal to a few percent and can be seen easily in fig.20. The RT reconstruction results for model 3 are represented in fig.21 (phase RT) end fig.22 (phase - difference RT). The experiment's geometry was taken to be the same as that of RATE-93 (h_0=1000km, τ_1=0km, τ_2=380.4km, τ_3=624.9km, τ_4=809.3km). As an initial guess we used here a very good approximation (fig.23) which in fact coincides with the background ionosphere. In spite of this good initial guess the phase method with the ART algorithm does not reveal the irregularity chain, whereas the phase-difference method does indentify the given structure quite satisfactority. Note that if the phase method is used with the MART algorithm, the irregularities can be isolated (fig.24). MART algorithms work better within the range of high values of the functions being reconstructed. However, this cannot be considered as an unconditional indication of MART algorithms being superior to ART ones. If, for example, a similar irregular structure of even a higher intensity $\Delta N=0.04*10^{12}m^{-3}$ (fig.25) is located at a greater altitude (at about 600km), i.e. not within the range of high values of the function being reconstructed, the MART algorithm begins distorting strongly the result (fig.26) in the attempt to "attach" such an irregular structure just inside the range of high

values of N, in other words, to attach the irregularities to the maximum of the layer. It goes without saying that such a distortion of results can lead to a wrong interpretation of the probing data and is undoubtedly a serious drawback of MART algorithms.

To summarize in brief the results of analysing various algorithms of solving SLE, it should be pointed out that at present it is not possible to say which algorithms have unconditional advantages over the othes, it seems to be impossible for all the cases of ionosphere RT. It is necessary to establish the conditions and areas of applicability for various methods and algorithms as soon as possible, therefore now there is a vast field for examining different combinations of algorithms as applied to problems of both phase and phase-difference RT. From our point of view, studies of methods to solve systems of equations [30-32] as applied to the ionospheric RT are also of interest. Mension should be made of the method using one-dimensional empirical orthonormal functions to reconstruct vertical ionospheric profile [30], the method based on the maximum entropy principle [31], a different orthogonal basis functions (whole domain functions) reconstruction algorithm [32]; several transform techniques [16,32]. Expansion into series in some continuous basis functions has both advantages and disadvantages. In our opinion, on the basis of our several years of experience in experimental RT reconstruction, one is most unlikely to find basis functions to describe adequately the variety of ionospheric processes. In order to obtain a resolution similar to that of discrete division, the number of basic functions must be of the same order as the number of discrete elements. Besides, the matrix of this problem would be less rarefied with a large condition

number and the method itself is highly sensitive to errors in the unknowns coefficients connected with high-order basic functions. Note the convenience of applying the methods [30-32] to the phase-difference problem have obvious advantages over the phase one. On the whole it should pointed out that at present there is no one preferable method to solve similar tomographic problems. Various methods may be better depending on the conditions of the experiment. It can be concluded from this that it is necessary to perform extensive research to test various methods and find the optimal methods as applied to specific ray RT schemes.

Here we shall not consider in detail the effects of the initial guess on the reconstruction results and make some brief remarks only. In simulations the uniform (in τ) ionosphere with different levels of the concentration maxima were used as an initial guess. Changes in initial guesses produce small changes in the background level, but the spatial structure of the local extrema remains the same. The spatial structure reconstructed by the phase-difference RT method can be said to weakly depend on the initial guess. Generally speaking, the aim is to generate an assembly of solutions satisfying (14) with a given accuracy determined by experimental errors. Now we have developed such methods of generating such solution assembly (by varying the algorithms, initial guess, etc.) which makes it possible to get an "assembly-averaged" solution and to estimate the reconstruction error distribution. This subject is, however, too extensive to be discussed in this paper.

3. Program <solve.for>

This program solves inverse problem for Phase RT or Phase-difference RT by means of different algorithms: ART, MART, SIRT. It calculates errors of reconstruction in metric C and L2 in dependence of data errors and noises.

Input parameters and files:

Parameters < Answer, NF, NR, NREC> are similar to same parameters of program <MATRIC.FOR>.

MOD.GRD - input file of model structure (program <INTEGR.FOR>)

XO.GRD - input file of initial guess (program <INTEGR.FOR>)

X - initial guess

Zmax - max value of initial guess

Function <GUESS> - for initial guess

RMAX, RM, Zmax, ZSM, B1, B2 - parameters for function <GUESS>

XIST - model structure from input file <MOD.GRD>

File <name_F.slv> containes the names of input and output files:

line 1 - name of file with parameters of matric (Fparam)

line 2: name1 - name of input file with matric

name2 - name of input file with either Phase or TEC or Doppler (output files (Fint) from program <INTEGR.FOR>)

name3 - name of output file with results of multiplications of input matric and reconstructed structure

Npi - array of contants (2πn) for each receiver

er_n - level of noise in %

Npi, er_n are introduced from the screen

Nsolve - the method of solution, it is introduced from the screen

REL - array of relaxation parameter

LMAX - max number of nonzero matric elements for each receiver

AZ - array of nonzero matric elements for all receivers

NST - array of corresponding column nonzero matric elements for all receivers

LST - array of number of all rays which cross the corresponding discret of model (SIRT algorithm) from input file <ST.dat>, it is similar to LST in program <MATRIC.FOR>

Niter - number of iterations, it is introduced from screen

Subroutine <DEFSYS> - solution of linear system equations for one ray.

Subroutine <ercl2> calculates errors in metric C and L2

Subroutine <VMINM> calculates min and max of array
Function <RAN> calculates random values in [0,1]
Output files:
File <REC.GRD> - the reconstruction
File <er-solv.dat> - errors of right items and reconstruction in metric C and L2
File <Fout> - results of multiplications of the matric and reconstructed structure
Execution
f77 solve.for
RUN
solve.exp

4. Analysis of the influence of data errors and noises on the reconstruction results.

Before presenting the results on the influence of errors in determining the absolute phase on the reconstruction results, let us estimate the possibilities of determining the absolute phase. The phase method involves measuring a linear integral of the form (1) multiplied by constant of the order of unity [2], which is insignificant here. The basis for difficulties appearing in the determination of the linear integral (6) is that the phase value is very high. For typical maximum values $N \sim 10^{12}$ m^{-3}, λ=2m and a ray length in the ionosphere of the order of a thousand kilometers, ϕ is thousands of radian. Thus, the problem arises of isolating the "initial phase" $\phi_0 = 2\pi n$, which must be added to the measured (within 2π) $\Delta\phi$ to obtain the complete phase $\phi = \phi_0 + \Delta\phi$ or the linear integral (6). To explain the difficulties arising, we will examine the possibility for isolating the initial phase in the presence of minor horizontal gradients.

We represent the concentration in the form of an expansion, where the regular spherically-symmetric background $N_0(r)$ is isolated $N(r,\alpha) = N_0(r) + N'(\alpha - \alpha_m)$, $N'(r) \equiv -\frac{\partial N}{\partial \alpha}\Big|_{\alpha=0}$; $\alpha_m(\phi)$ is

the angle of intersection of the ionospheric maximum by the ray; its vicinity makes the primary contribution to integral (6). In this case, retaining the first terms of the expansion in terms of powers h/R in (6), we obtain

$$\phi \simeq \frac{\lambda r_e}{\cos\phi} \int N_0(h)dh - \lambda r_e \frac{tg^2\phi}{\cos\phi} \int \frac{h}{r} N_0(h)dh +$$

$$+ \frac{\lambda r_e}{\cos\phi} \int N'(h)(\alpha(h)-\alpha_m)dh + \ldots \qquad (22)$$

If there were no horizontal gradient, it might be possible to measure $\Delta\phi(\psi)$ for various angles ψ in the range $\Delta\psi$ and obtain a system of linear equations from which it would be possible to determine $\int N_0 dh$, $\int dh\ h\ N_0/R$ etc. In other words, the known functional dependence on ψ would make it possible to isolate the TEC and other moments of the function $N_0(h)$. However, the presence of the term with N' greatly complicates the situation when its value becomes comparable to 2π. We will estimate this term in the case of nearly vertical sounding $|\alpha|$, $|\alpha_i| \ll 1$; for this, in the integrand we replace $\alpha(h) - \alpha_m$ by $\psi(h-h_m)/(R+h) \simeq \psi(h-h_m)/R$, h_m is the height of the maximum; this asymptotic equation follows (at low angles) from (4): $\psi \simeq (\alpha-\alpha_i)/(1-R/r) = (\alpha-\alpha_i)(R+h)/h$. Therefore, such methods for isolating the constant component will be suitable under the condition

$$\left|\lambda r_e \Delta\psi \int \frac{N'(h)(h-h_m)}{R} dh\right| \ll 2\pi. \qquad (23)$$

The typical values of $\partial N/\partial\alpha$ in the presence of a "trough" in the ionosphere $\partial N/\partial\alpha \sim 10^{13}$ m^{-3} radian^{-1}, then (23) is only satified for $\Delta\psi \ll 10^{-2}$. However, at angles of fractions of a degree it is practically impossible to determine the functional dependence on ψ in the presence of noises. Inequality (23) applies

to the case of determination of the TEC along the vertical. The limitation on the horizontal gradient becomes even more strict in oblique sounding. A detailed analysis of a number of traditional techniques for determination the constant phase was provided in [33]. These techniques include combined techniques Doppler and Faraday measurements simultaneously. The results of numerical modeling [33] showed that in the presence of a trough and characteristic gradients $\partial N/\partial\alpha \sim 10^{13}$ м$^{-3}$ radian^{-1} the error in determination of the constants varies within 100-1000%! This agrees with estimate (23) and indicates that practical determination of the linear integral of the electron concentration is unrealistic in the presence of characteristic horizontal gradients in the ionosphere, while it is specifically this case which is of interest for RT.

There is one more method for determining the TEC in the presence of horizontal gradients [34-36] which is based on recording of satellite signals at a pair of separated receiving stations. With data on the phases on a fixed base, it is possible to compare the pair of linear equations with the nearly identical last terms of (22), i.e., the rays traveling to different receivers should intersect the ionospheric maximum at one point. Likewise, a pair of equations for another moment in time leads to a system for the initial phase, in which the influence of the gradient term will be reduced. Otherwise, condition (23) is replaced by a less strict condition. However, it is impossible to completely eliminate the influence of horizontal gradient and subsequent derivatives on the result of determination of the initial phase by a such a method. The methods used [28-30] have an error by constant of about 10% or at least a few percents. Of course, it is always possible to propose a variant of the

recording method in which it is possible to determine the initial phase; but to do so, one must perform a multifrequency reception using an array of several receivers.

Thus, by virtue of the nature of the phase measurements, it is inadvisable to reduce the problem of ionospheric RT to a problem in linear integrals. Determination of initial phase by the simplest recording systems leads to major errors, while the use of complex multiposition and multifrequency systems is not justified here, since a different solution of the problem is possible by the phase-difference or Doppler measurements without determination of the initial phase.

Here are the results of numerical simulation of the reconstruction of the ionosphere section for typical errors in finding the absolute phase (TEC). A simple model of the ionosphere with a trough and a positive inhomogeneity at the left edge of the trough (model 1) is used for numerical simulation. It was assumed that satellite radio probing (h_0=1000 km) was performed at the frequencies 400 and 150 MHz (λ=2m) and the receivers are located at the points with the coordinates τ_1=0 km, τ_2=475 km, τ_3=1435km. A homogeneous ionosphere having no trough was used as a initial guess Fig.27. Fig.28 and Fig.29 show the results of the reconstruction with the help of the phase RT with $\pm$3% and $\pm$5% accuracy in determing the TEC (which corresponds the error in the value of the absolute of 6π and 10π), the signs of the errors don't coincide for different receivers. These figures illustrate an extremely poor quality of reconstruction using the phase RT method with typical errors in determining the TEC: even the principal features of this simple model structure are not recovered and at the same time some heavy artefacts are present. Fig.30 shows the dependences of the reconstruction errors δ_2

and δ_∞ on the error in determining the absolute phase ($\pm 2\pi m$), on the number m. It can be seen that even errors of a few units 2π lead to a poor quality of reconstruction. It should be noted that if the SIRT algorithm is used, as it was done by other authors in [12,17,19], rather than the ART algorithm, the reconstruction results similar to those in Figs.28-29 will at first sight be better. They have a more regular, less "chaotic" character. The averaging SIRT algorithms result in the reconstruction being weaker dependent on measurement errors, i.e. the SIRT algorithms are less sensitive to small variations of data and therefore poorly reflect the fine structure of the reconstructed cross-sections. The SIRT algorithms can reconstruct the general background quite satisfactorily but often they fail to reveal even the existing trough if it is 20-40% smaller than the maximum. If the signs of the errors in determining the absolute phase are the same for all the receivers, the reconstruction quality is somewhat better. Nevertheless at the level of errors greater then 10%, the reconstruction quality is still poor. In Fig.31 we represent the result of reconstruction of the model 1 using the phase-difference RT method (the matrix was built by piecewise-planar approximation). One can easily see that the principal features of the ionosphere section are reconstructed quite well. Numerical simulation of the reconstruction of various ionospheric structures carried out by us proved a noticeable advantage of the phase-difference RT method over the phase RT with typical errors in determining the absolute phase.

Note another significant limitation of RT methods connected with deviation of receivers from the satellite flight plane. Similar deviation can also lead to significant errors in determining the absolute phase. Let us introduce the distance p in

the direction perpendicular to this plane, and the deviation angle $tg\gamma=p/L$ where L is the (tilted) distance to the satellite. Then it can easily be shown that the difference between the phase detected by the receiver in the flight plane and that detected by receiver off the plane by p will be:

$$\Delta\phi \simeq \lambda r_e N_t(1/\cos\gamma - 1) + \lambda r_e \sin\gamma \langle \partial N/\partial p \rangle L^2/2 \qquad (24)$$

where $\langle \partial N/\partial p \rangle = \frac{2}{L^2} \int_0^L \left.\frac{\partial N}{\partial p}\right|_{p=0} ldl$ - the ray "averaged" transverse gradient of the electron density, N_t is the TEC along the ray. The correction associated with changing tilted distance (the first summand in (24)) can easily be taken into account. However, strong transverse gradients can noticeably change the phase, and for the phase method the following condition must be satisfied:

$$\lambda\, r_e \sin\gamma \left\langle \frac{\partial N}{\partial p} \right\rangle \frac{L^2}{2} \ll 2\pi \qquad (25)$$

with the typical gradient $\langle \partial N/\partial p \rangle \sim 10^5$ m^{-4} and distances $L \sim 10^6$m, this fact results in a strict limitation of $p \ll 10$km. However this limitation was not taken into account in the experiments [17,19,20]. The sheme of experiment [17] seems to be strange and surprising because the Kaliningrad-Riga-Leningrad track makes an angle of the order of 45^0 with the satellite trajectory projection. The angle between Kiruna-Oulu direction [19] and the satellite trajectory projection is also greater then 40^0. Note that the deviation of the receiver from the satellite plane only due to the Earth's rotation during the recording time of the order of 10 minutes can reach a hundred kilometers in the middle latitudes, which is quite significant for phase RT. For the

phase-difference RT it is only relative smallness of the change $\Delta\phi$ in respect to the basic phase that is required, which leads to the inequality $\langle\partial N_t/\partial p\rangle p \ll N_t$ that is practically always fulfilled.

Consider the influence of the noise-type errors on the reconstraction results. The physical origin of such noises may be connected both with instrumental errors and external noises. Methods of phase-difference RT provide quite satisfactory results even with considerable errors in experimental data. Fig.32 shows the reconstruction by the method of phase-difference RT, but in this case the data with the noise level being 10% of maximum amplitude of Doppler data were used. One can see that random measurements errors slightly affect the reconstruction results, almost there is no defference between Fig.31 and Fig.32. This conclusion is confirmed by fig.33 showing the dependence of the reconstruction error in the l^2 metrics on the noise level. Even the 50% noise level changes the reconstruction error only slightly, which can be explained by mutual compensation and effective "averaging" of noises in the process of tomographic reconstruction. In the phase-difference RT experiments [24,27-29]the noise level does not exceed a few percent. The results of the simulation also show that the influence of noises on the phase RT method is rather weak, because within the frame work of this model it is possible to consider weak noises within the 2π-innternal only, which amounts to 10^{-3} in typical ionospheric conditions. Thus, for the phase RT method, errors in determining the "initial phase" are of paramount importance and it is difficult to avoid such errors due to numerous factors, such as horisontal gradients, deviations of receivers from the plane of recording, changes in the position of receivers owing the Earth's rotation, etc.

References

1. V.E.Kunitsyn, E.D.Tereshchenko, "Radio Tomography of the Ionosphere", Antennas & Propagation Magazine, Vol.34, 22-32,1992.
2. V.E.Kunitsyn, E.D.Tereshchenko, *Tomography of the Ionosphere*, Nauka, Moscow, 1991 (in Russian).
3. K.Dines, J.Lytle, "Computerized geophysical tomography, Proc.IEEE, V.67, 1065-1073, 1979.
4. S.Ivansson, "Seismic borehole tomography - theory and computational methods", Proc.IEEE, V.74, 328-338, 1986.
5. *Seismic Tomography*, Ed.by G.Nolet, Reidel.Publ.Comp., Dordrecht, 1987.
6. R.S.Spindel, "Ocean acoustic tomography. A new measuring tool", Oceanus, V.25, 12-21, 1982.
7. W.H.Munk, C.Wunsch, "Ocean acoustic tomography: rays and modes", Rev.Geophys.Space Phys., V.21, 777-793, 1983.
8. R.A.Phinney, D.L.Anderson, "On the radio occultation method for study planetary atmospheres", J.Geophys.Res., V.73, 1819 - 1827, 1968.
9. V.P.Aksenov, V.A. Banakh, E.A.Efimova et al. "Reconstruction of 2D Fields of Atmospheic Parameters from Lidar Signals Reflected by the Earth's Surface", Optics of Atmosphere, V.4, No 10, 1061-1065, 1991 (in Russian).
10. P.E.Krasnushkin, "Tomographic methods of research high frequency radiowave propagation around Earth", Dokl.Akademy of Science USSR, V.257, 1099-1102, 1981.
11. P.E.Krasnushkin, "Determination of Earth distribution of parameters of HF propagation on the inclined probing by means of tomographic method", Geomagetizm and Aeronomy, V.21, 1133-1135, 1981.
12. R.J.Austen, S.J.Franke, C.H.Liu, "Ionospheric imaging using computerized tomography", Radio Science, V.23, 299-307, 1988.
13. E.L.Afraimovich, O.M.Pirog, A.I.Terekhov, "Diagnostic of large-scale structures of the high lalitude of the ionosphere by means of tomographic processing navigation satellites signals and data of ionosonds", Preprint Sib.IZMIR, No 19-89, Irkutsk, p.1-12, 1989 (in Russian).
14. M.Gustavsson, S.Ivansson, P.Moren et al.,"Seismic borehole tomography - measurement system and field studies", Proc.IEEE, V.74, 339-346, 1986.
15. T.D.Raymond, R.J.Austen, S.J.Franke, et al., "Application of computerized tomography to the investigation of ionospheric

structures", Radio Science, V.25, 771-789, 1990.
16. K.C.Yeh, T.D.Raymond, "Limitations of ionospheric imaging by tomography", Radio Science, Vol.26, pp.1361-1380, 1991.
17. Y.S.Saenko, I.I.Shagimuratov, A.N.Namgaladze, et al., "Reconstruction of electron density distribution in the ionosphere based on the tomographic processing of satellite radio signals, Geomagnetizm and Aeronomy, V.31, 558-561, 1991.
18. E.L.Afraimovich, O.M.Pirog, A.I.Terekhov, "Diagnostics of large-scale structures of the high-latitude ionosphere based on tomographic treatment of navigation satellite signals and of data from ionospheric stations", J.Atm.Terr.Phys., V.54, 1265-1273, 1992.
19. S.E.Pryse, L.Kersley, "A preliminary experimental test of ionospheric tomography", J.Atm.Terr.Phys., V.54, 1007-1012, 1992.
20. S.E.Pryse, L.Kersley, D.L.Rice, et al., "Tomographic Imaging of the ionospheric mid-lalitude trough", Ann.Geophys., V.11, 144-149, 1993.
21. T.D.Raymond, S.E.Pryse, L.Kersley, et al., "Tomographic reconstruction of ionospheric electron density with European incoherent scatter radar verification", Radio Science, V.28, 811-817, 1993.
22. J.A.Klobuchar, P.F.Fougere, P.H.Doherty, "The Promise and the Potential Perils of Ionospheric Tomography", Abstracts IEEE/AP-S Symposium, London, Canada, p.544, 1992.
23. M.Kunitake, Hayakawa M., Ohtaka K. et al. "Ionospheric Tomography campaign May-July 1992 in Japan, Abstracts of XXIV Gen. Assem. of the URSI, Kyoto, p.330, 1993.
24. V.E.Kunitsyn, E.D.Tereshchenko, E.S.Andreeva et al., *Radiotomography of global ionospheric structures*, Preprint Polar Geophys.Inst., 90-10-78, pp.1-30, 1990 (in Russian).
25. V.L.Ginzburg, *Propagation of electromagnetic waves in plasma*, Gordon and Breach, Science Publishers, Inc., NY, 1961.
26. E.S.Andreeva, V.E.Kunitsyn, "Simulation of tomographic reconstruction artificial ionospheric lens", Proc. III Suzdal URSI Symp. on Modification of the Ionosphere by Powerful Radio Waves, 127-128, Moscow, 1991.
27. V.E.Kunitsyn, E.D.Tereshchenko, "Radio Tomography of the Ionosphere", Antennas & Propagation Magazine, Vol.34, 22-32,1992.
28. E.S.Andreeva, A.V.Galinov, V.E.Kunitsyn et al., "Radiotomographic reconstruction of ionization trough in the plasma near the Earth", J.Exp.Theor.Phys. Lett., V.52, 145-148, 1990.
29. E.S.Andreeva, V.E.Kunitsyn, E.D.Tereshchenko, "Phase difference radiotomography of the ionosphere", Annales Geophys.,

V.10, 849-855, 1992.

30. E.J.Fremow, J.A.Secan, B.M.Howe, "Application of stochastic inverse theory to ionospheric tomography", Radio Sci., V.27, 721-732, 1992.
31. P.F.Fougere, "Ionospheric tomography using the maximum entropy technique, Proc. Int. Beacon Satell.Symp., p.125-128, 1992.
32. H.Na, H.Lee, "Orthogonal decomposition technique for ionospheric tomography", Int.J.Imaging Syst.Technol., V.3, 354-365, 1991.
33. G.K.Solodovnikov, V.M.Sinelnikov, E.B.Krokhmalnikov, *Remote sounding of the Earth ionosphere by the satellite beacons*, Nauka, Moscow, 1988 (in Russian).
34. R.Leitinger, G.K.Hartman, F.J.Lohman, et al. "Electron content measurements with geodetic Doppler receivers", Radio Sci., V.19, 789 - 797, 1984.
35. R.Leitinger, G.Schmidt, A.Taurianen, "An evaluation method combining the differential Doppler measurements from the station that enables the calculation of the electron content of the ionosphere", J.Geophys., V.41, 201 - 213, 1975.
36. G.F.Lyon, G.A.Fulford, A.Forsyth, "Ionospheric effects on space application system", Canadian. Aeronaut. Space, V.29, 315 - 326, 1983.

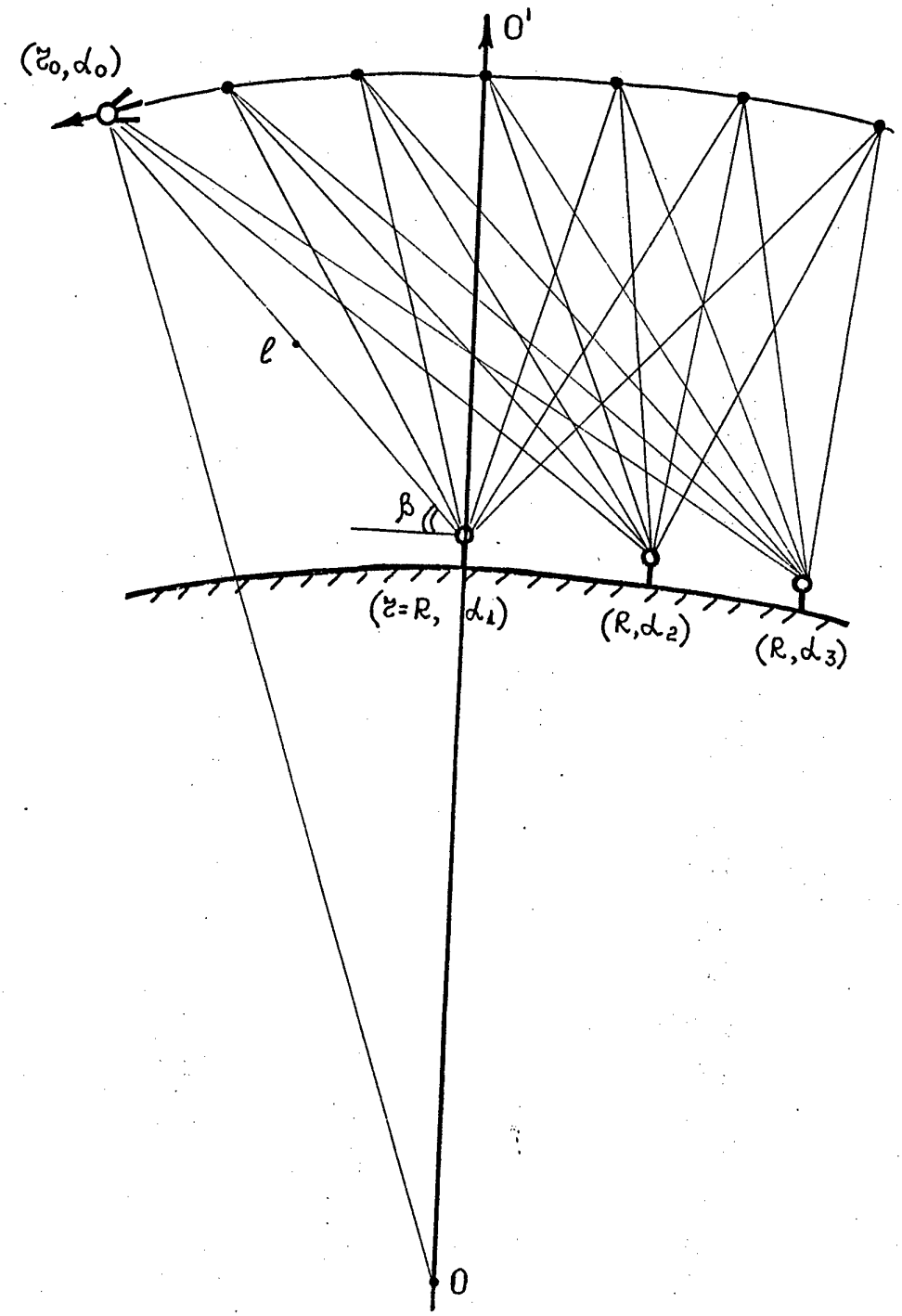

Fig. 0

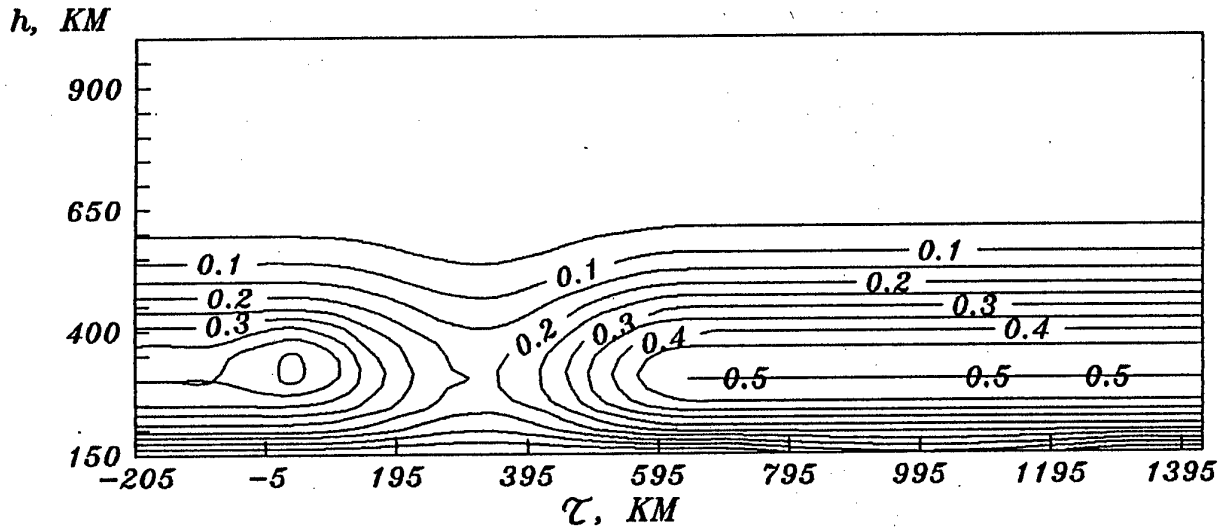
h, KM
900
650
400
150
0.1
0.2
0.3
0.4
0.5
−205
−5
195
395
595
795
995
1195
1395
τ, KM

Fig. 1

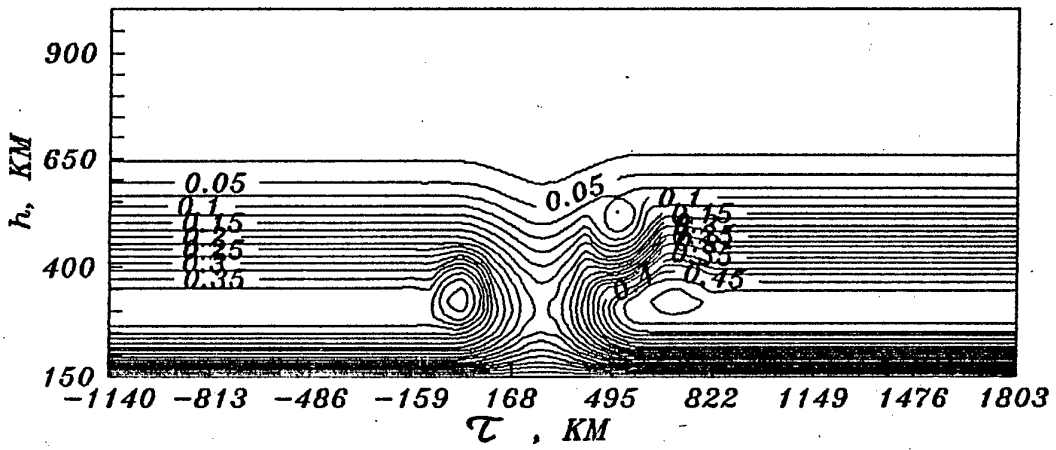
900
650
400
150
h, KM
0.05
0.1
0.15
0.25
0.35
0.05
0.1
0.45
−1140 −813 −486 −159 168 495 822 1149 1476 1803
τ , KM

Fig. 2

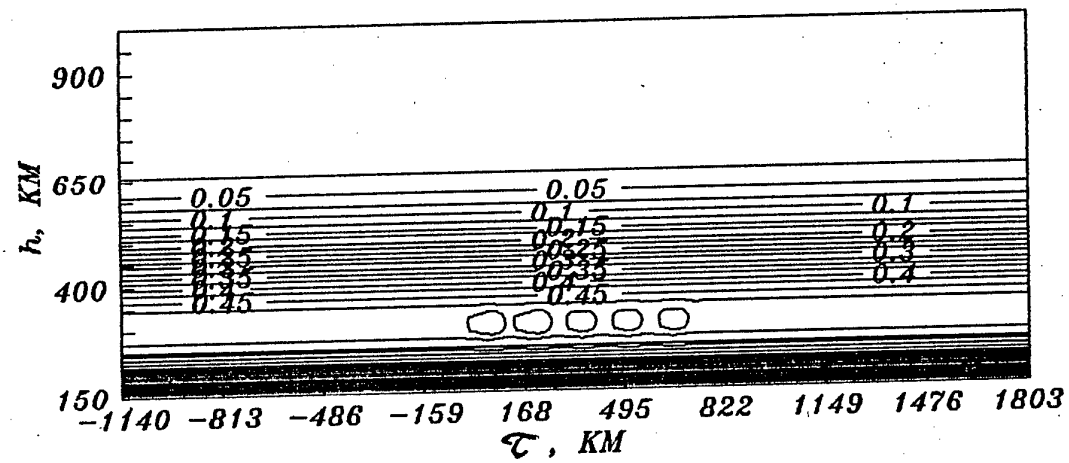
900
650
400
150
h, KM
0.05
0.1
0.15
0.25
0.35
0.45
0.05
0.1
0.15
0.25
0.35
0.45
0.1
0.2
0.3
0.4
-1140
-813
-486
-159
168
495
822
1149
1476
1803
τ, KM

Fig. 3

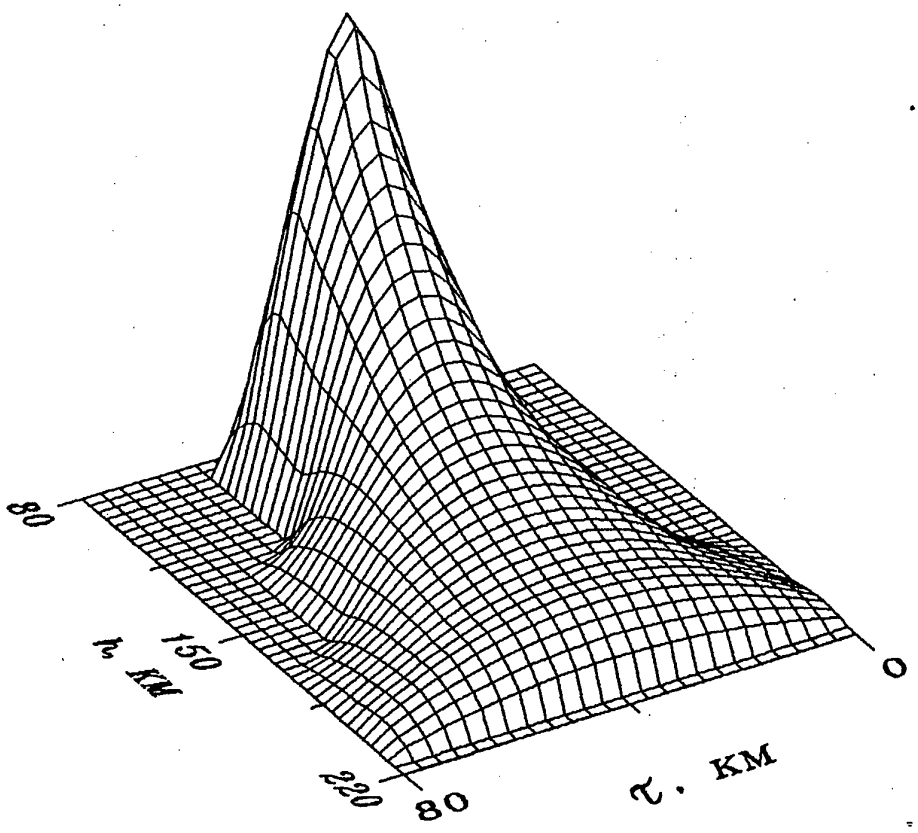

Fig. 4

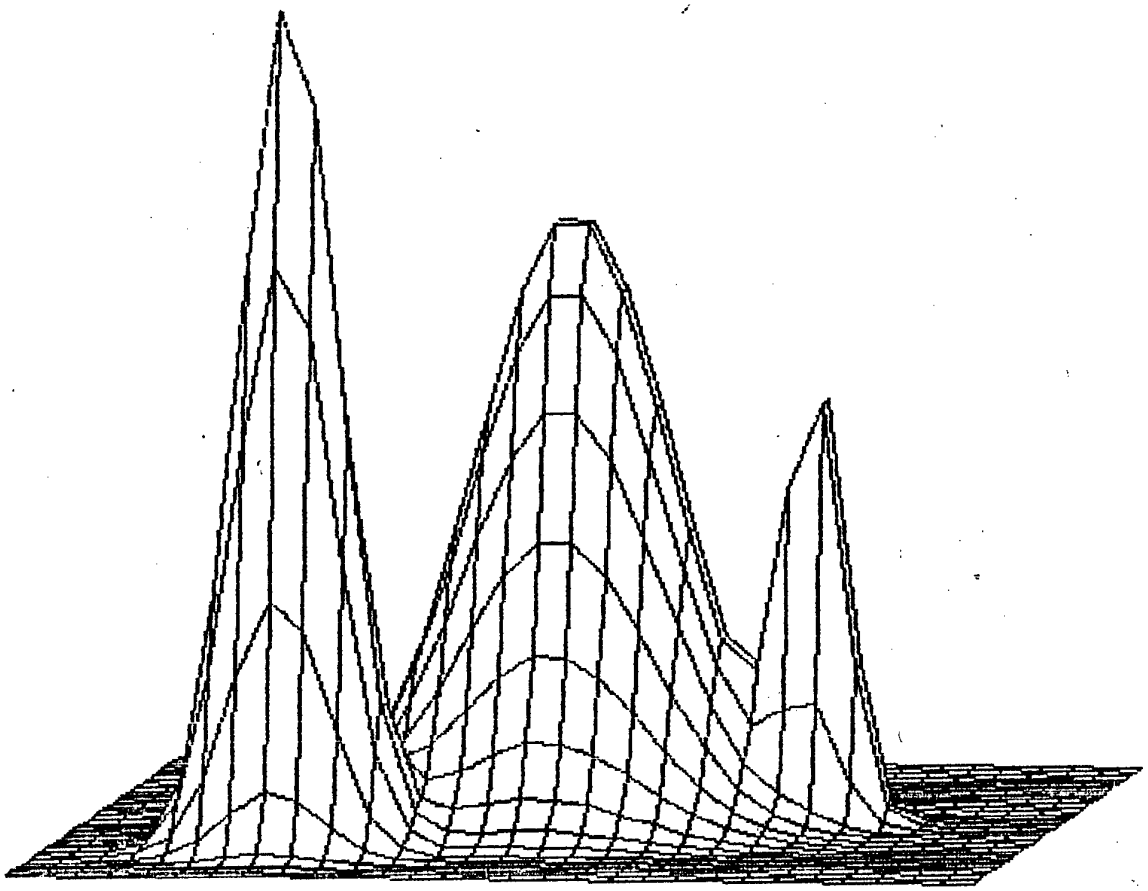

Fig. 5

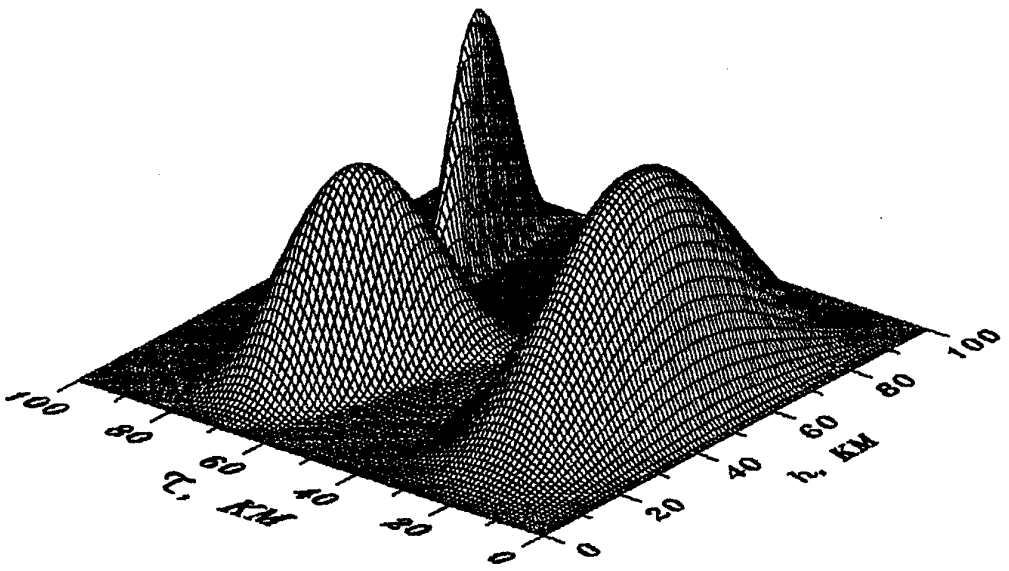

Fig. 6

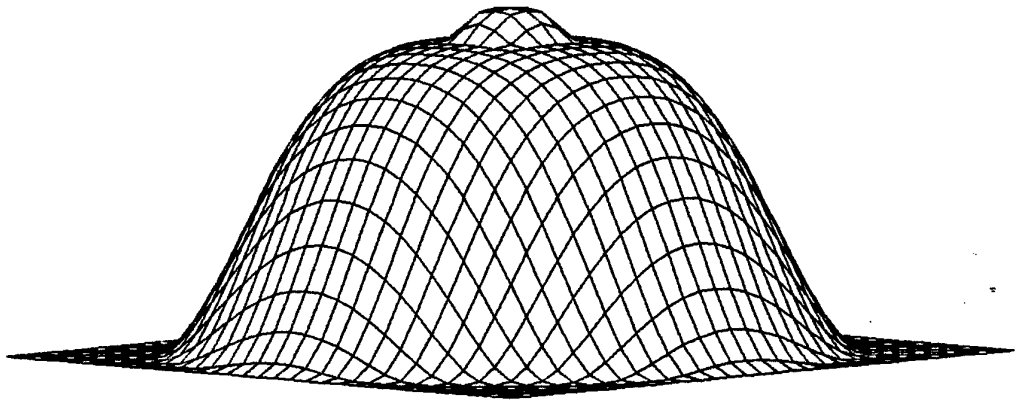

Fig. 7.

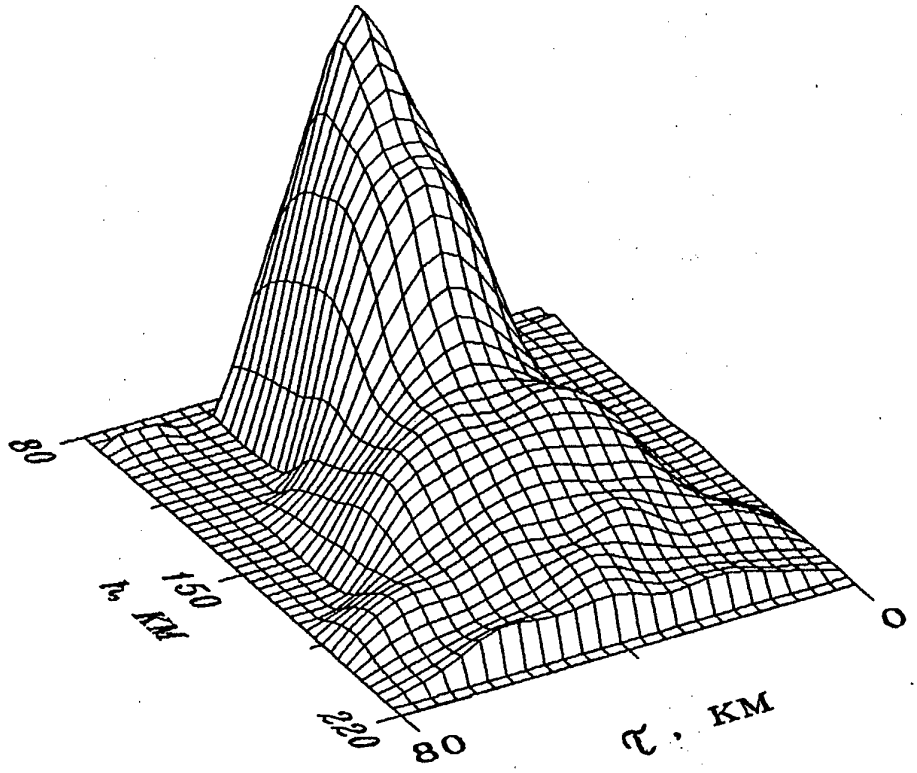

Fig. 8

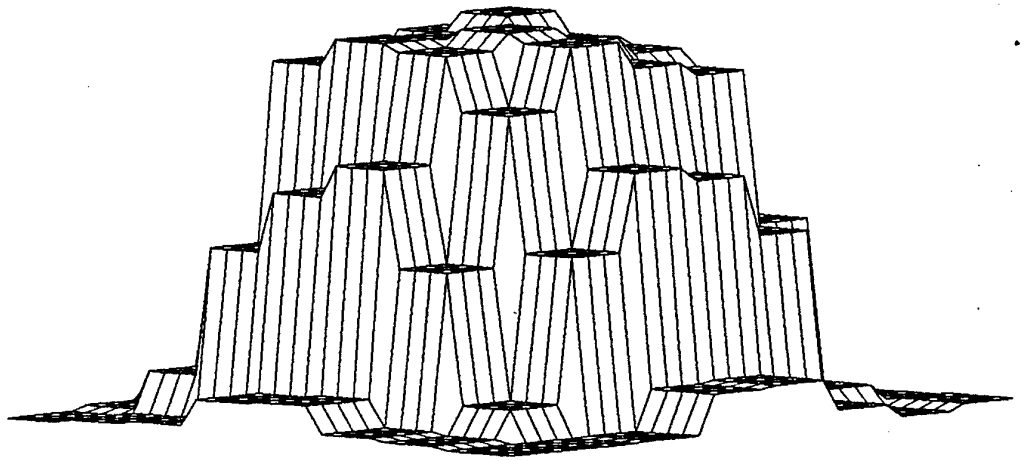

Fig. 9 (A)

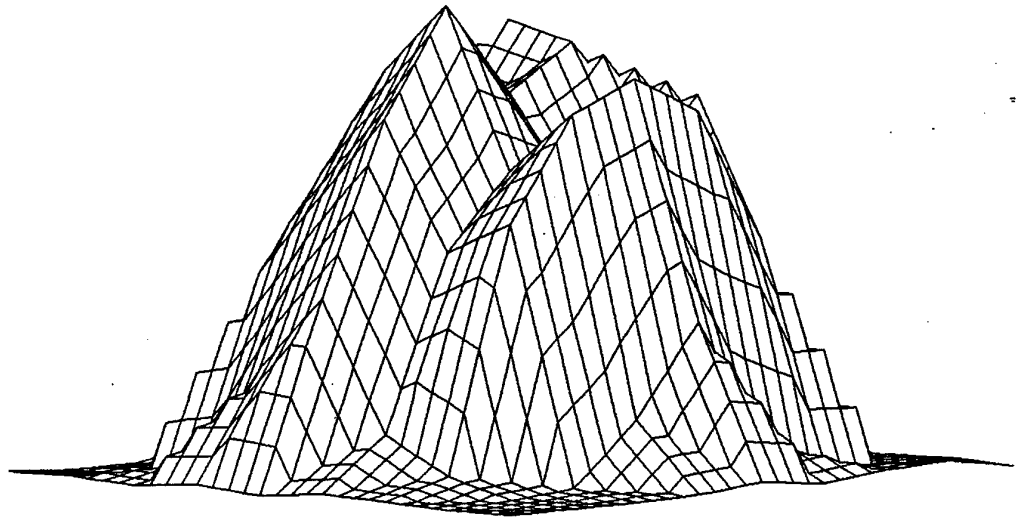

Fig. 9 (B)

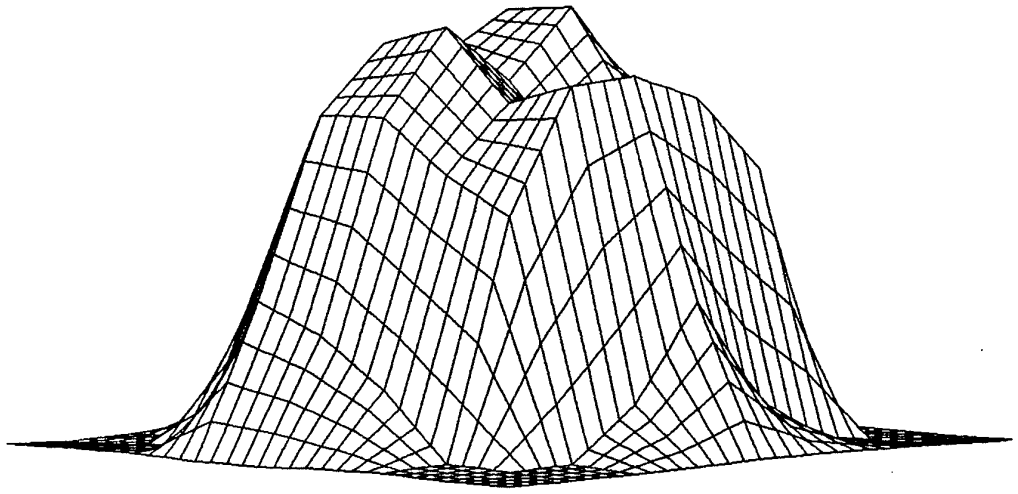

Fig. 9 (C)

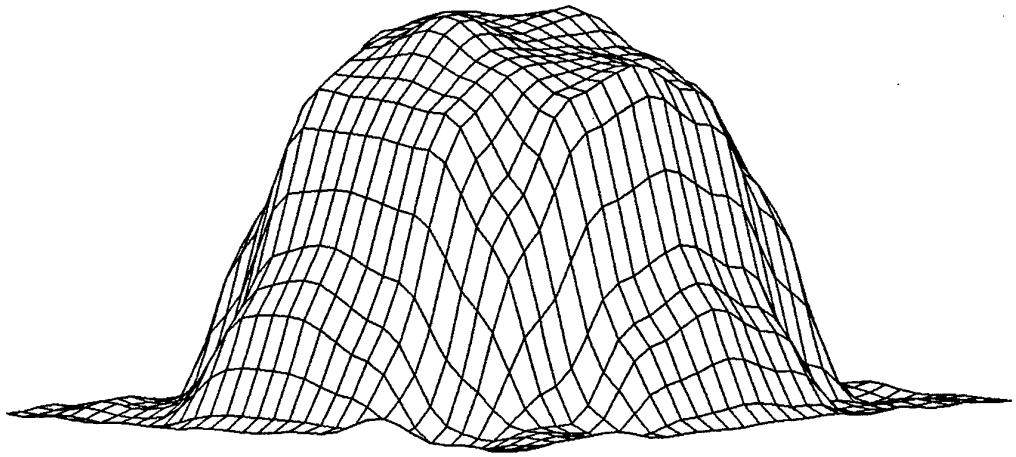

Fig. 9 (D)

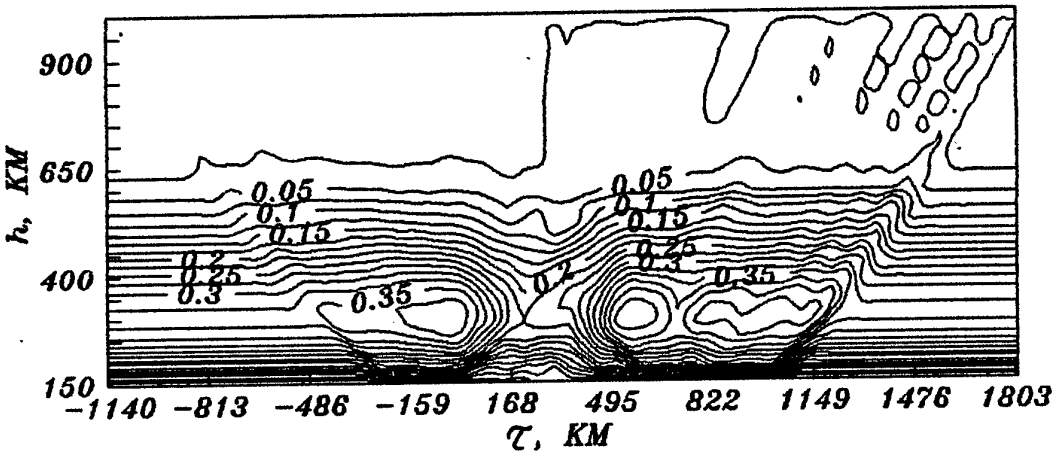
900
650
400
150
h, KM
0.05
0.1
0.15
0.2
0.25
0.3
0.35
−1140 −813 −486 −159 168 495 822 1149 1476 1803
τ, KM

Fig. 10 (B)

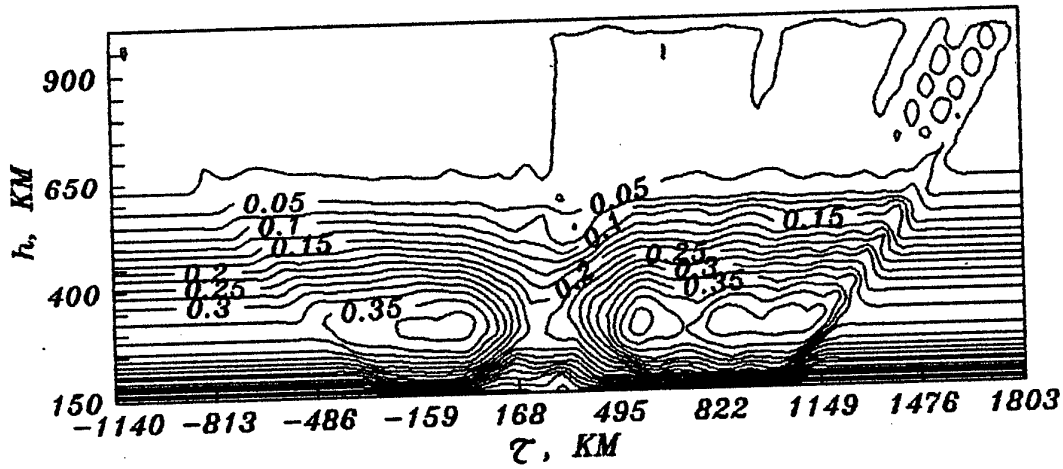
900
650
400
150
h, KM
0.05
0.1
0.15
0.2
0.25
0.3
0.35
−1140 −813 −486 −159 168 495 822 1149 1476 1803
τ, KM

Fig. 10 (c)

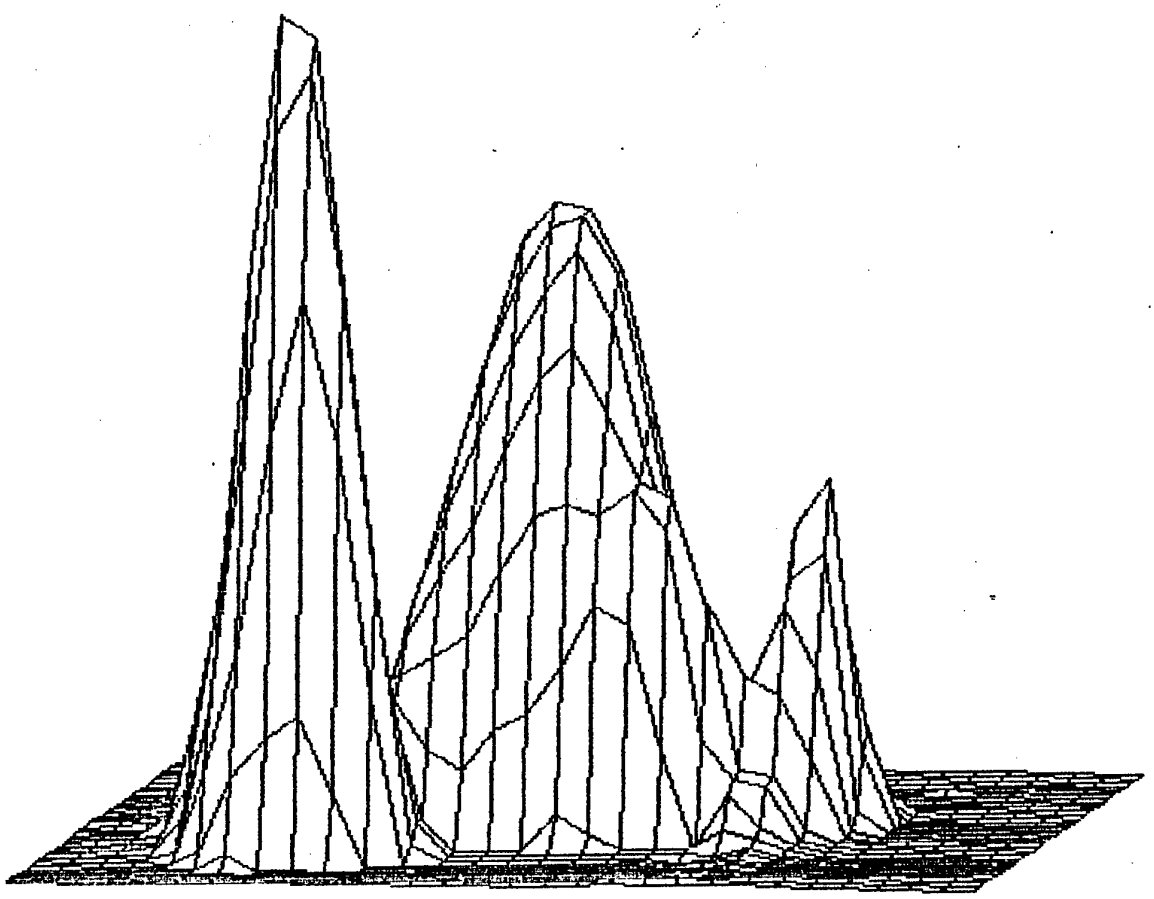

Fig. 11

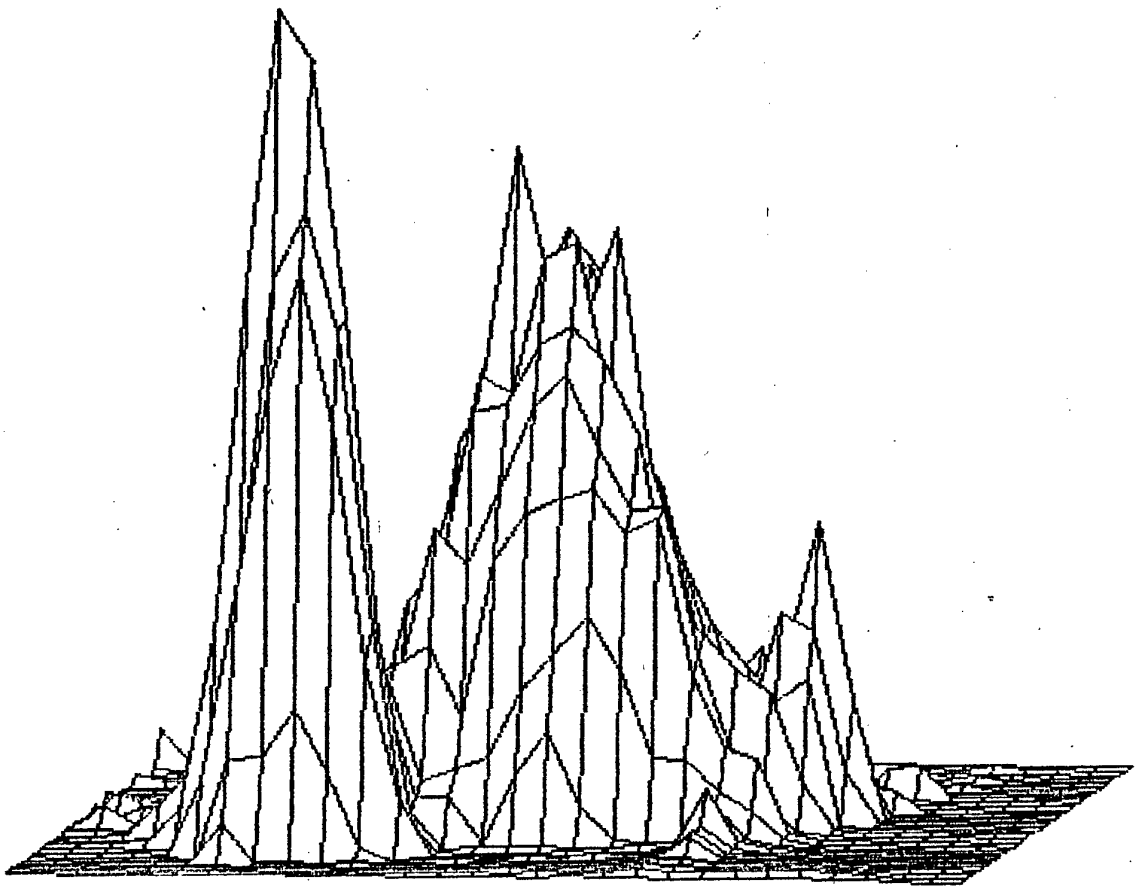

Fig. 12

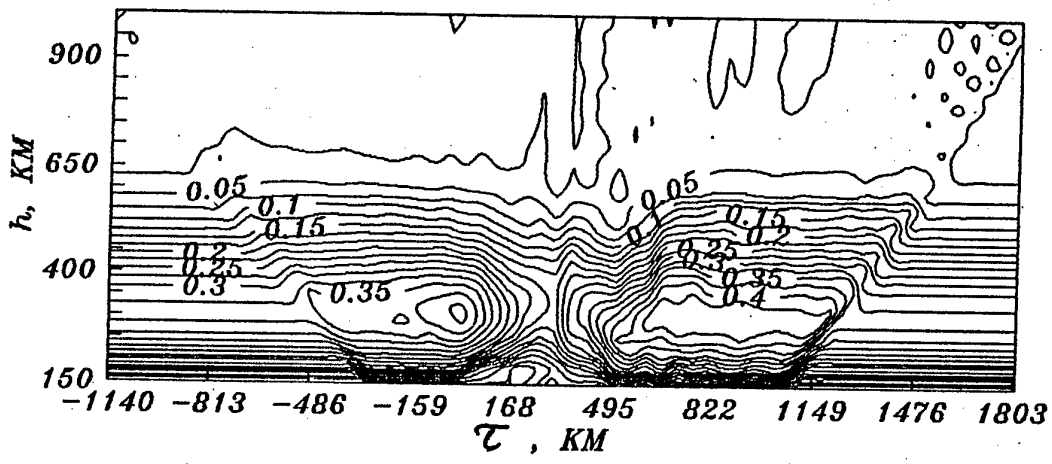
900
650
400
150
h, KM
0.05
0.1
0.15
0.2
0.25
0.3
0.35
0.4
−1140 −813 −486 −159 168 495 822 1149 1476 1803
τ , KM

Fig. 13

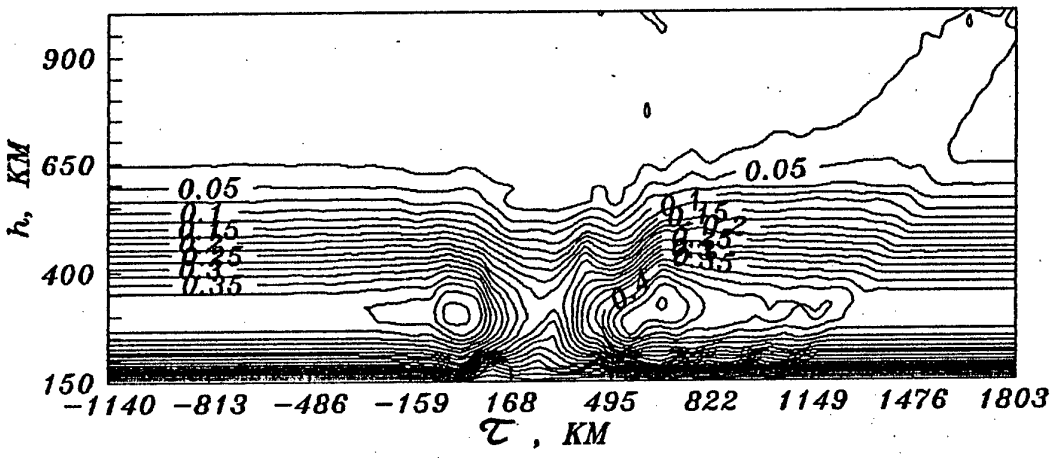
900
650
400
150
h, KM
0.05
0.05
0.1
0.15
0.2
0.25
0.3
0.35
0.4
−1140 −813 −486 −159 168 495 822 1149 1476 1803
τ , KM

Fig. 14

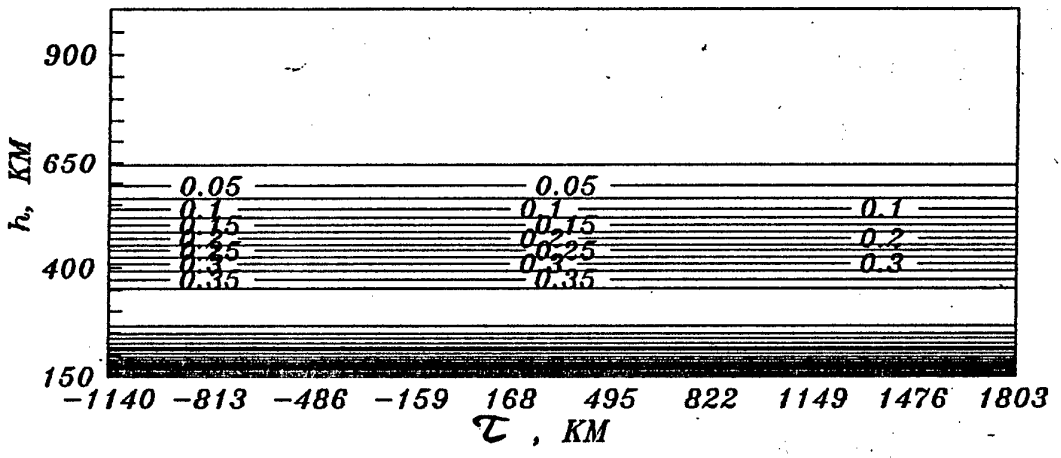
900
650
400
150
h, KM
0.05
0.1
0.15
0.2
0.25
0.3
0.35
0.05
0.1
0.15
0.2
0.25
0.3
0.35
0.1
0.2
0.3
−1140 −813 −486 −159 168 495 822 1149 1476 1803
τ , KM

Fig. 15

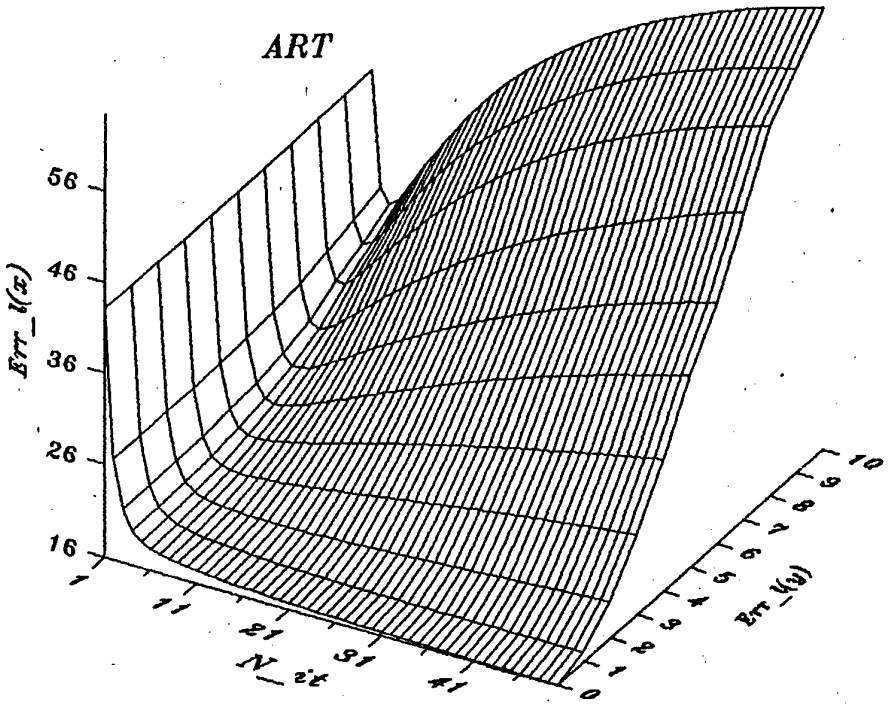

Fig. 16

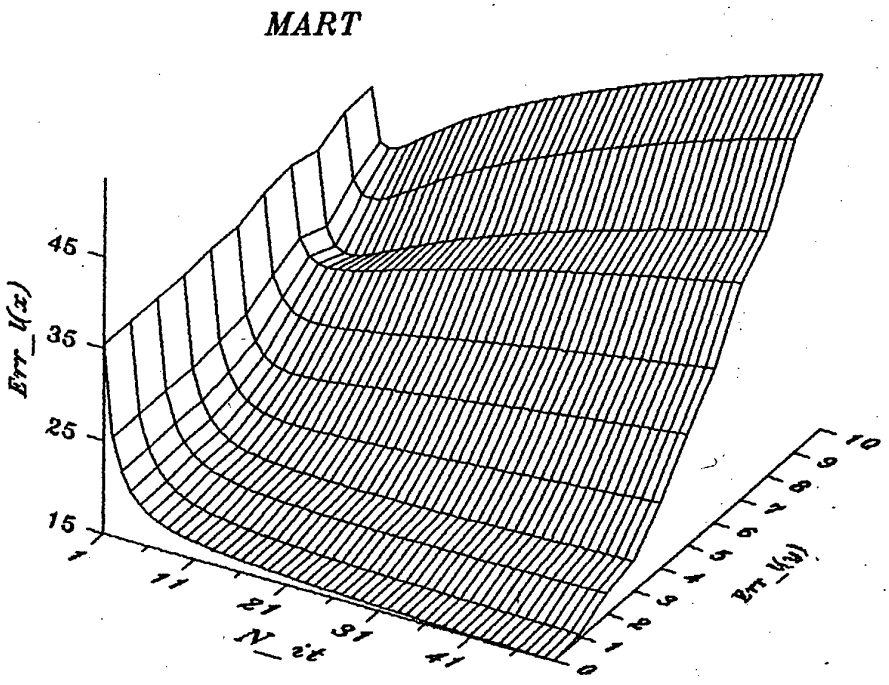

Fig. 17

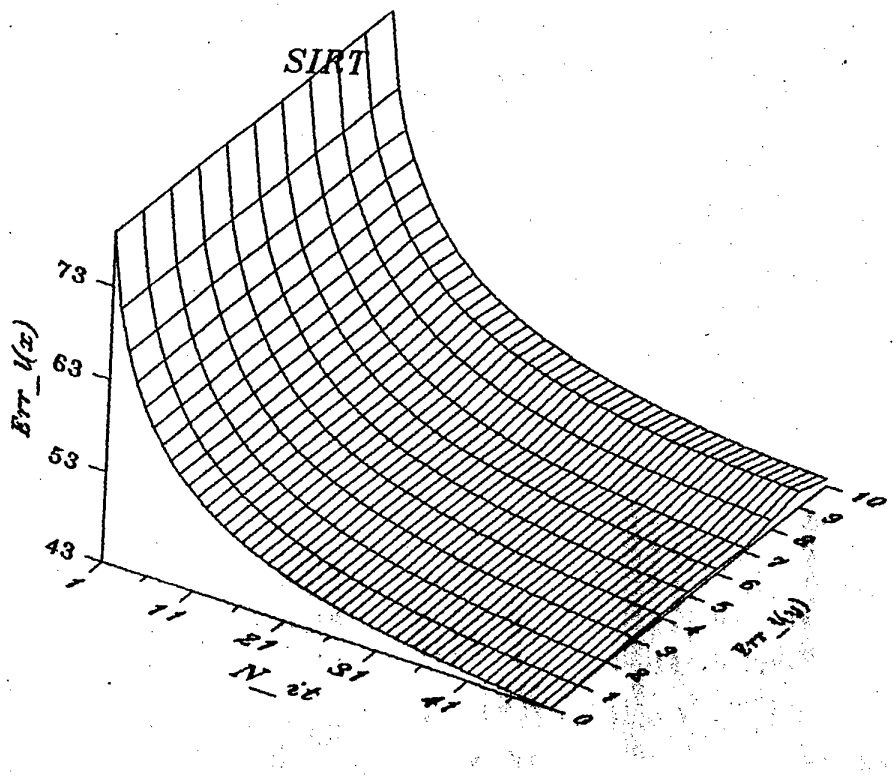

Fig. 18

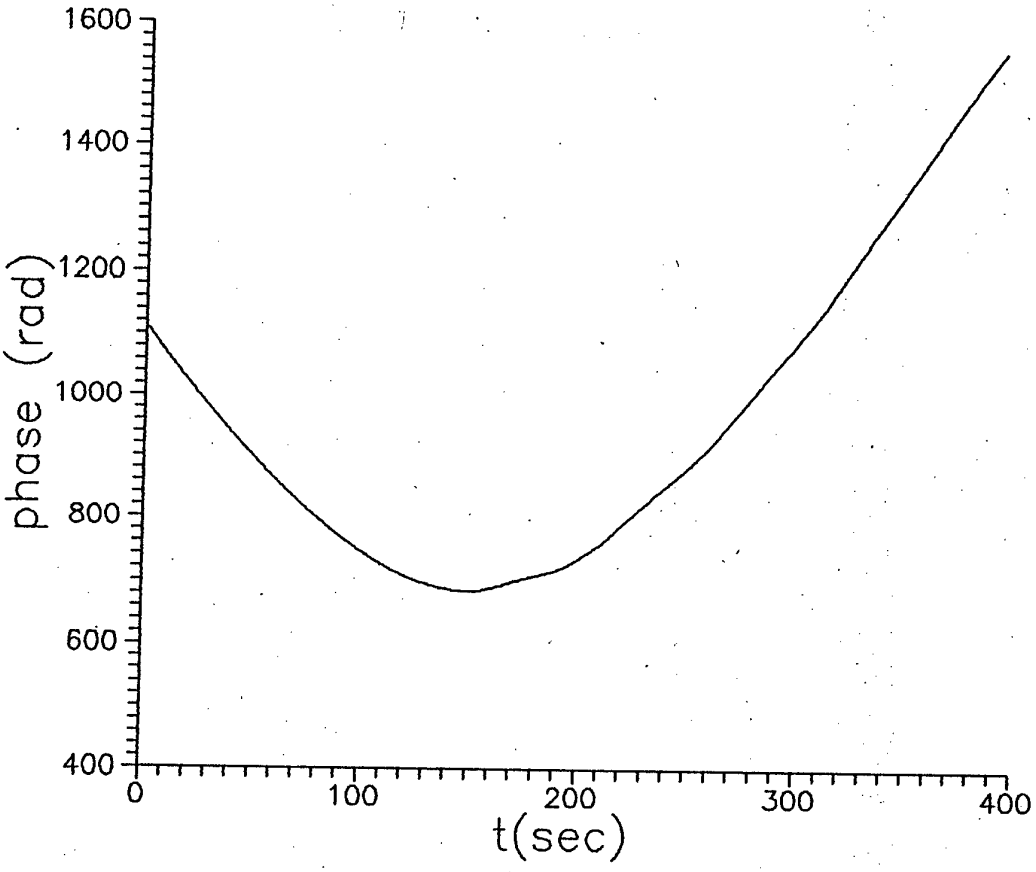
1600
1400
1200
1000
800
600
400
phase (rad)
0
100
200
300
400
t(sec)

Fig. 19

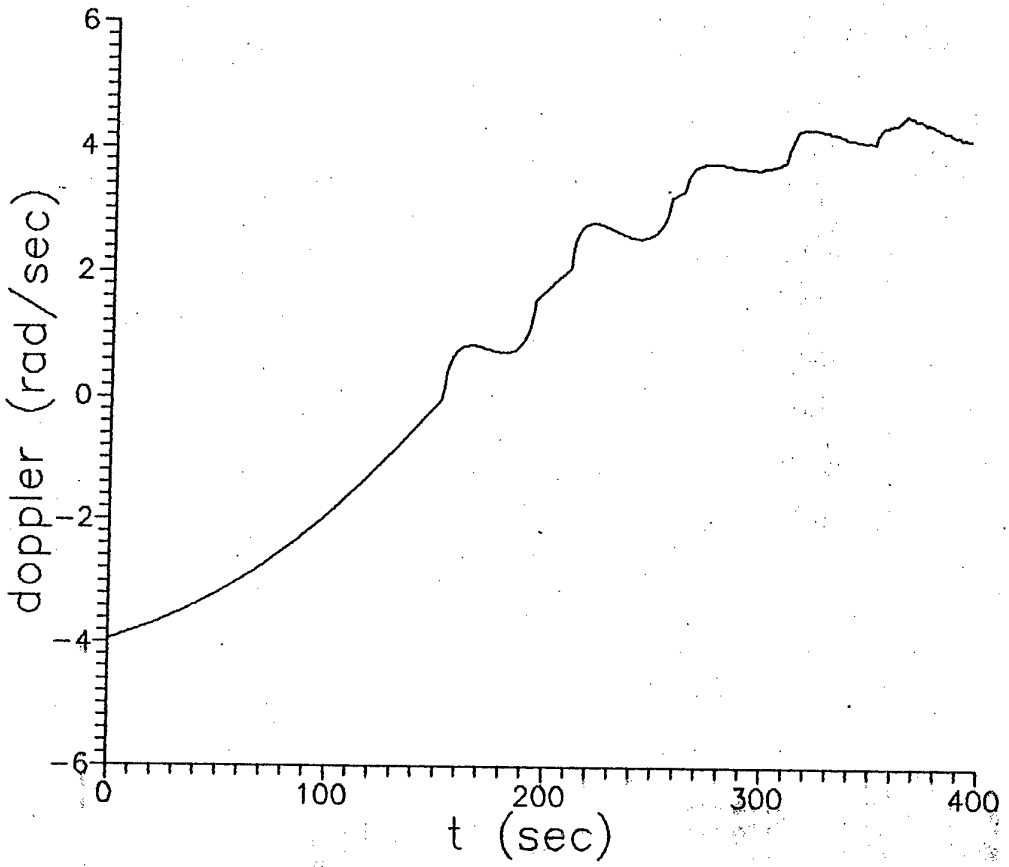

Fig. 20

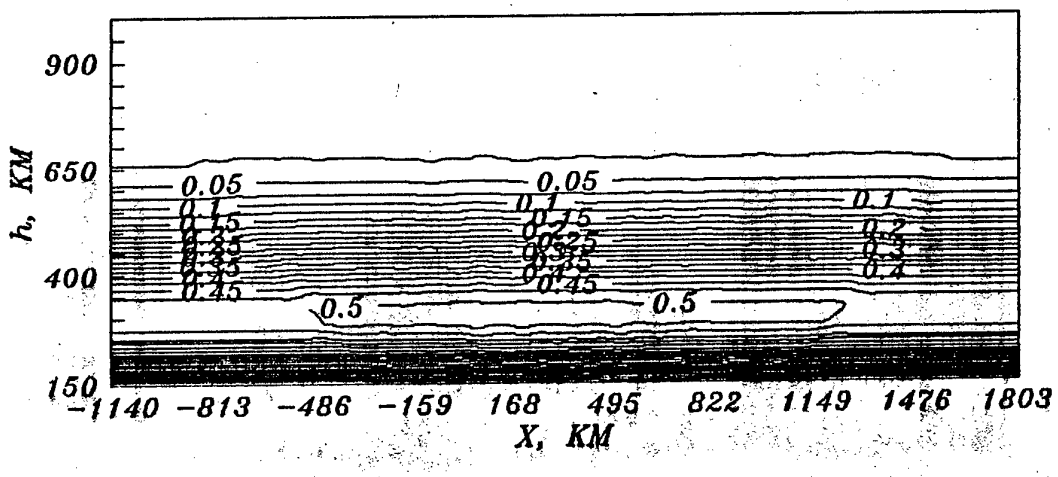
900
650
400
150
h, KM
0.05
0.1
0.15
0.2
0.25
0.3
0.35
0.4
0.45
0.5
−1140 −813 −486 −159 168 495 822 1149 1476 1803
X, KM

Fig. 21

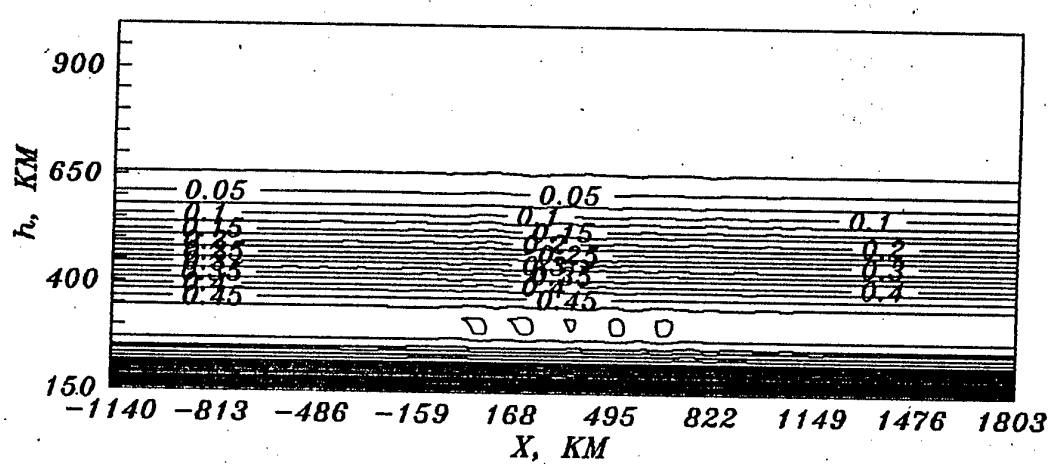
900
650
400
150
h, KM
0.05
0.1
0.15
0.25
0.45
0.4
−1140 −813 −486 −159 168 495 822 1149 1476 1803
X, KM

Fig. 22.

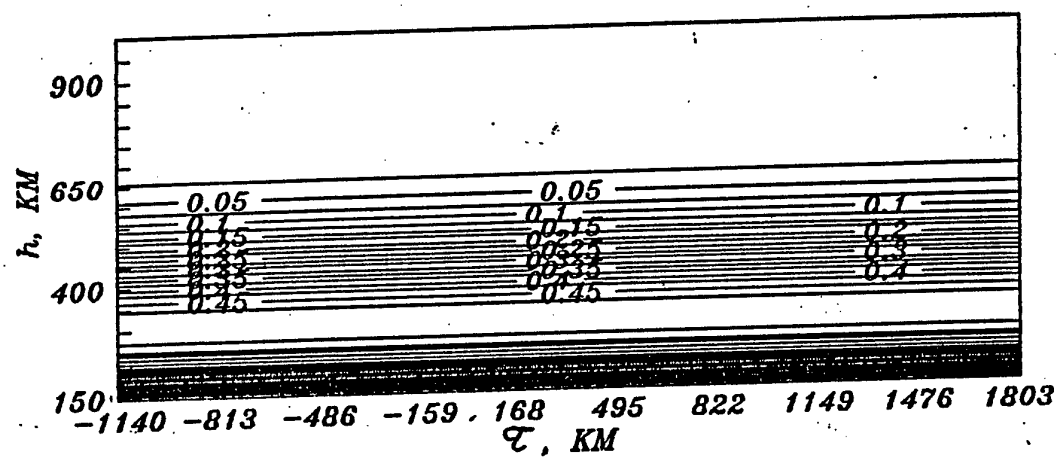
900
650
400
150
h, KM
0.05
0.1
0.15
0.25
0.35
0.45
0.2
0.3
0.4
−1140
−813
−486
−159
168
495
822
1149
1476
1803
τ, KM

Fig. 23

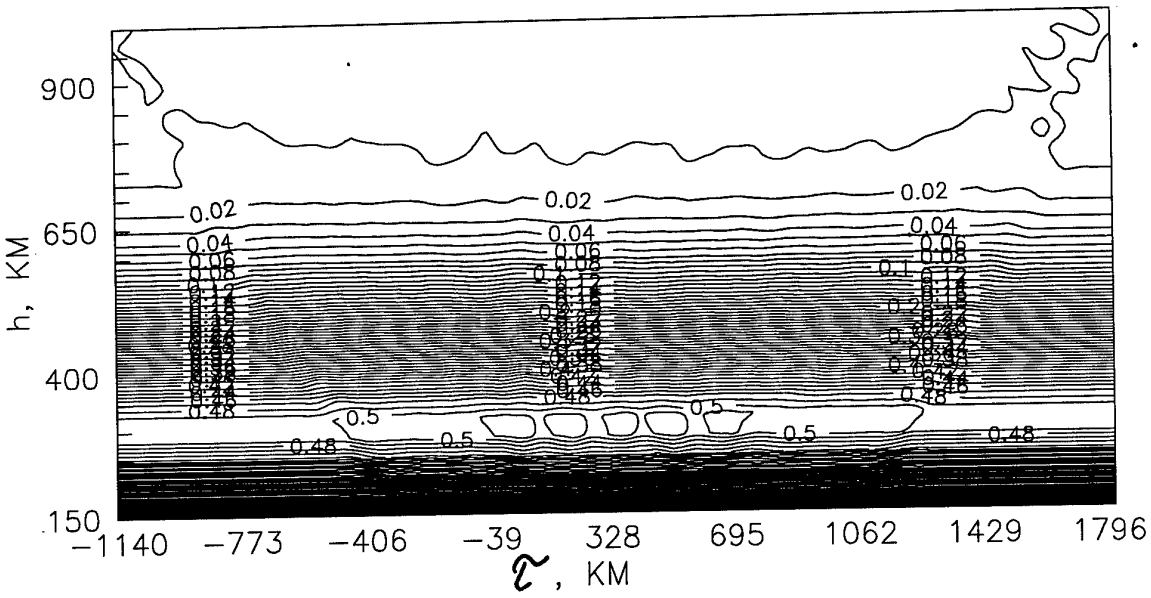
900
650
400
150
h, KM
0.02
0.04
0.06
0.08
0.1
0.48
0.5
−1140
−773
−406
−39
328
695
1062
1429
1796
τ, KM

Fig. 24

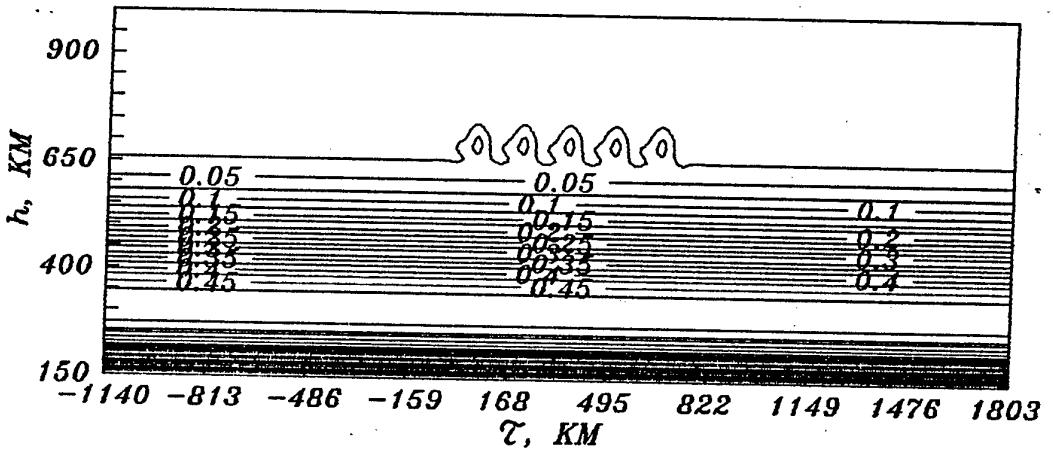
900
650
400
150
h, KM
0.05
0.1
0.15
0.2
0.25
0.3
0.35
0.4
0.45
−1140 −813 −486 −159 168 495 822 1149 1476 1803
τ, KM

Fig. 25

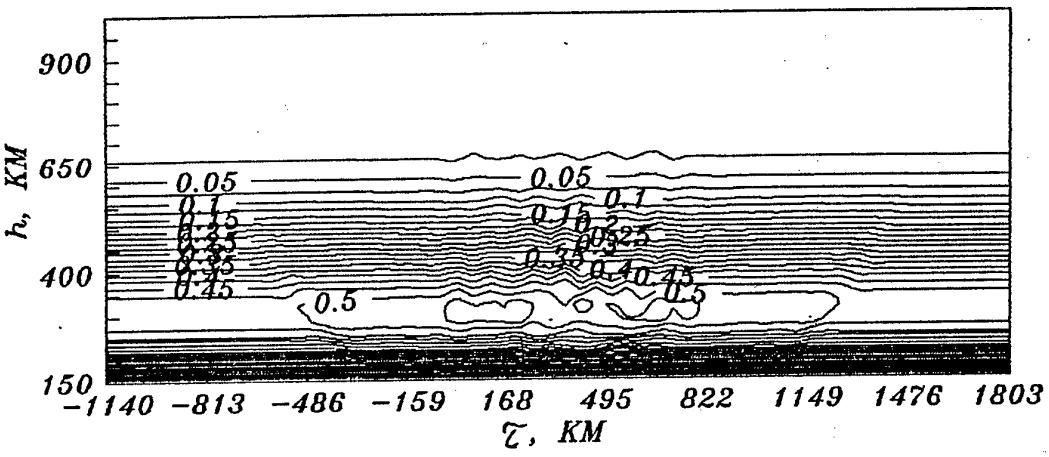
900
650
400
150
h, KM
0.05
0.1
0.5
−1140 −813 −486 −159 168 495 822 1149 1476 1803
τ, KM

Fig. 26

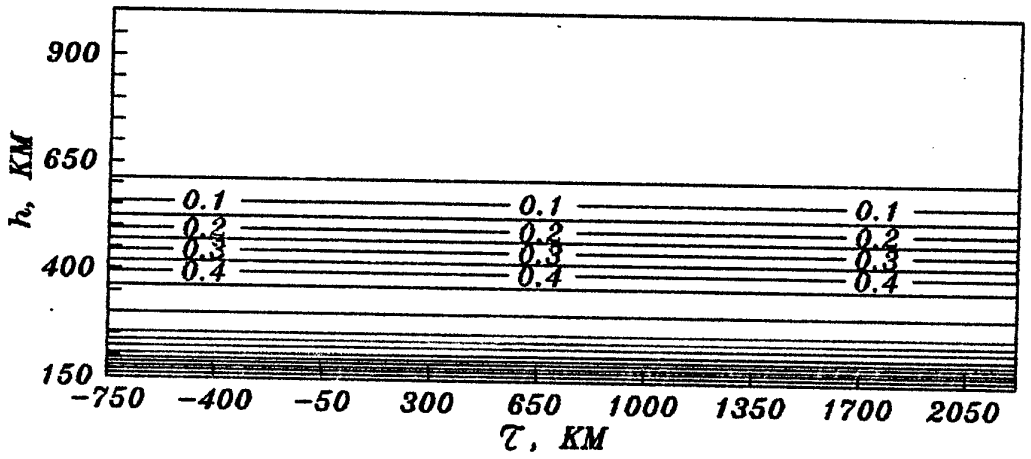
900
650
400
150
h, KM
0.1
0.2
0.3
0.4
0.1
0.2
0.3
0.4
0.1
0.2
0.3
0.4
-750
-400
-50
300
650
1000
1350
1700
2050
τ, KM

Fig. 27

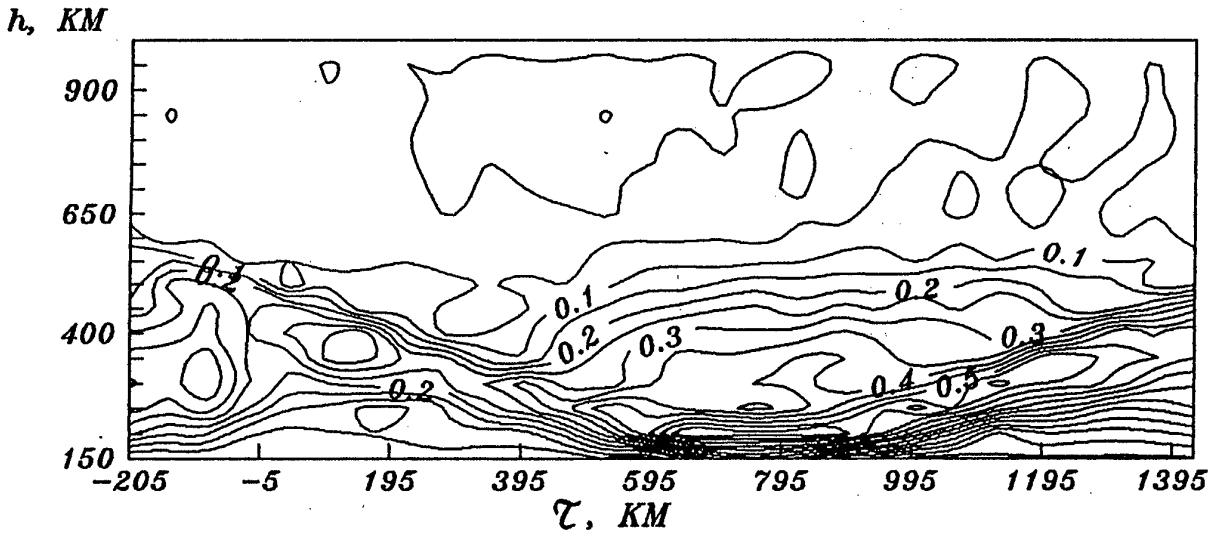
h, KM
900
650
400
150
0.1
0.2
0.3
0.4
0.5
−205
−5
195
395
595
795
995
1195
1395
τ, KM

Fig. 28

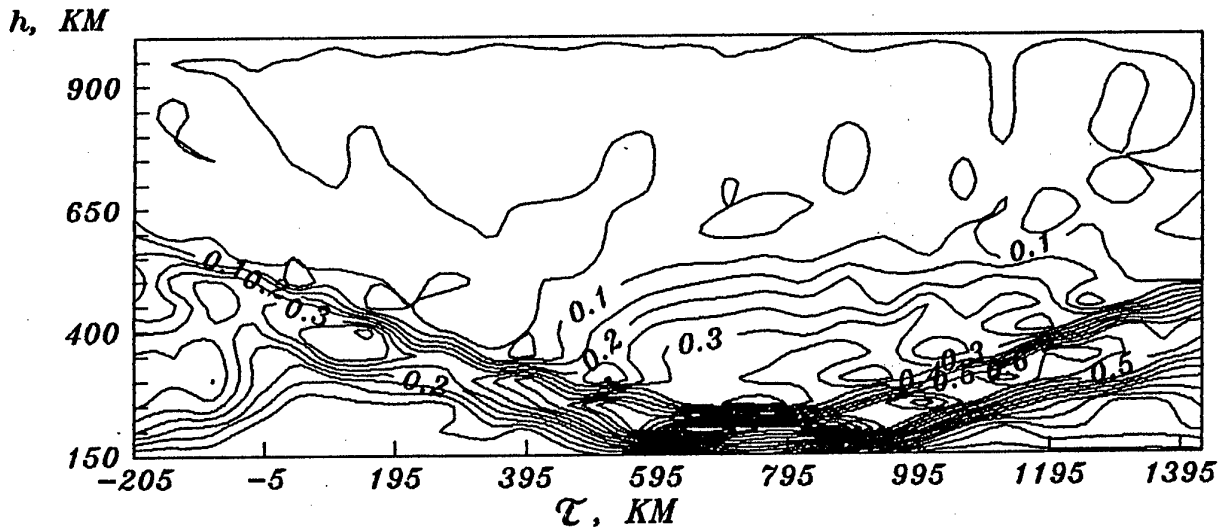
h, KM
900
650
400
150
0.1
0.2
0.3
0.5
−205
−5
195
395
595
795
995
1195
1395
τ, KM

Fig. 29

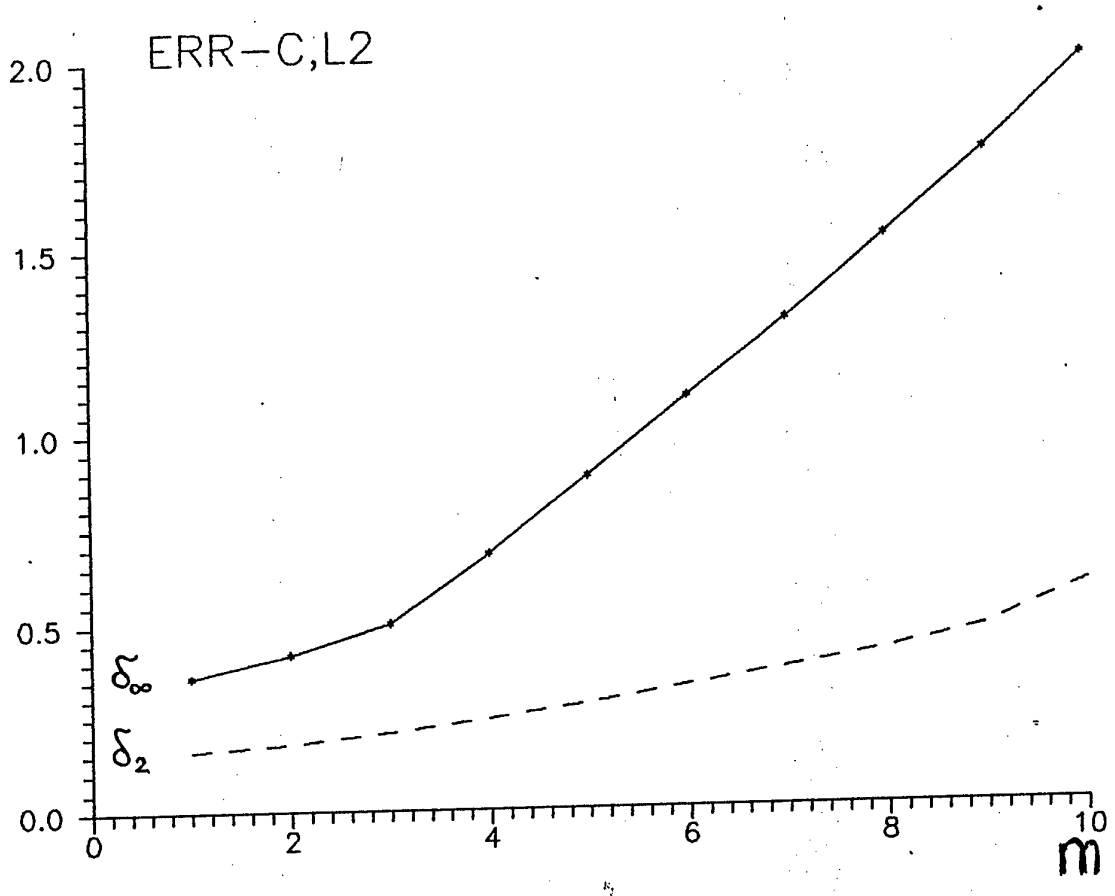

Fig. 30

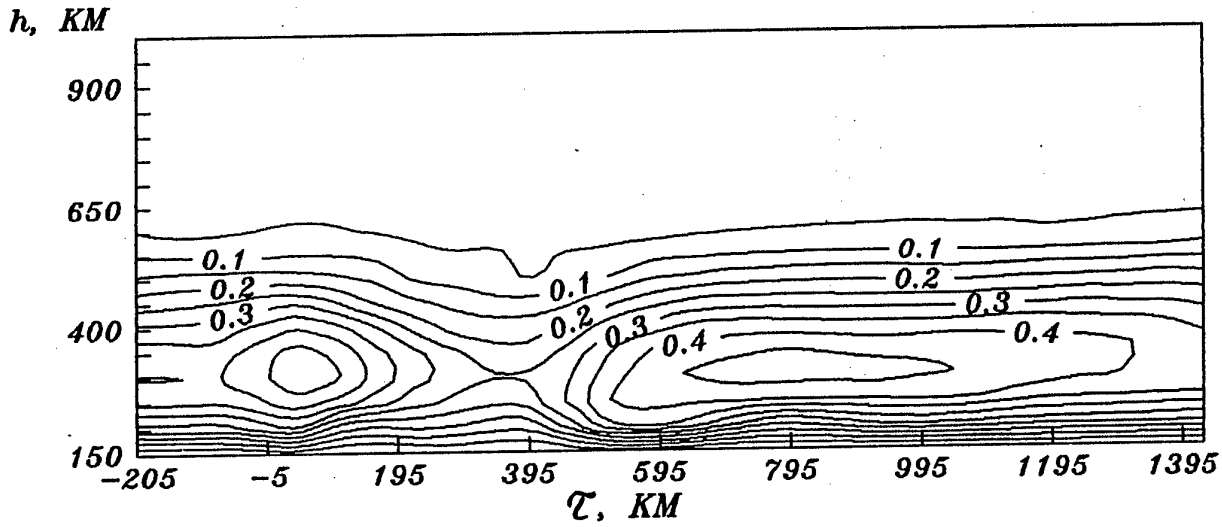
h, KM
900
650
400
150
0.1
0.2
0.3
0.1
0.2
0.3
0.4
0.1
0.2
0.3
0.4
−205
−5
195
395
595
795
995
1195
1395
τ, KM

Fig. 31

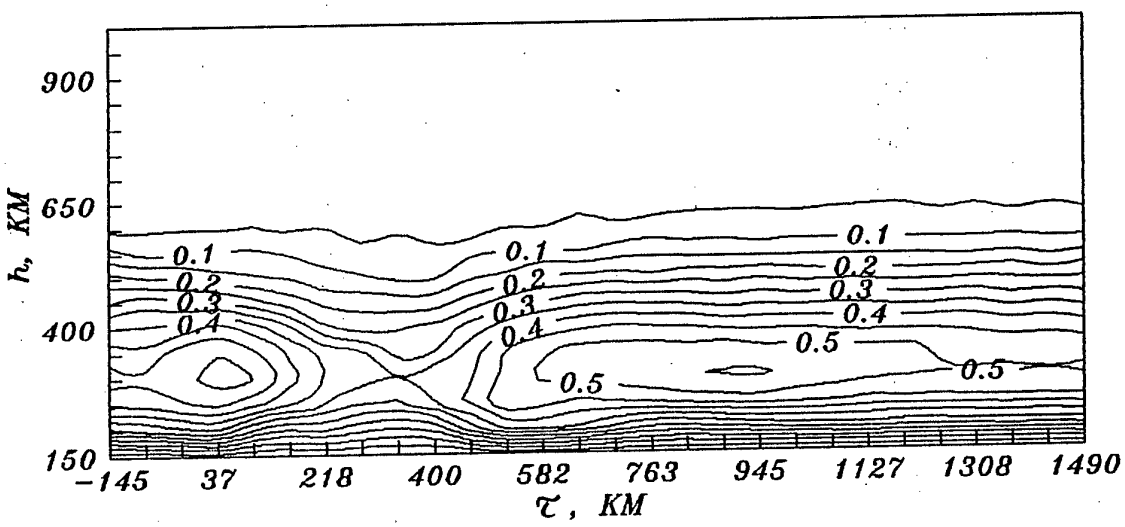
900
650
400
150
h, KM
0.1
0.2
0.3
0.4
0.5
−145
37
218
400
582
763
945
1127
1308
1490
τ, KM

Fig. 32

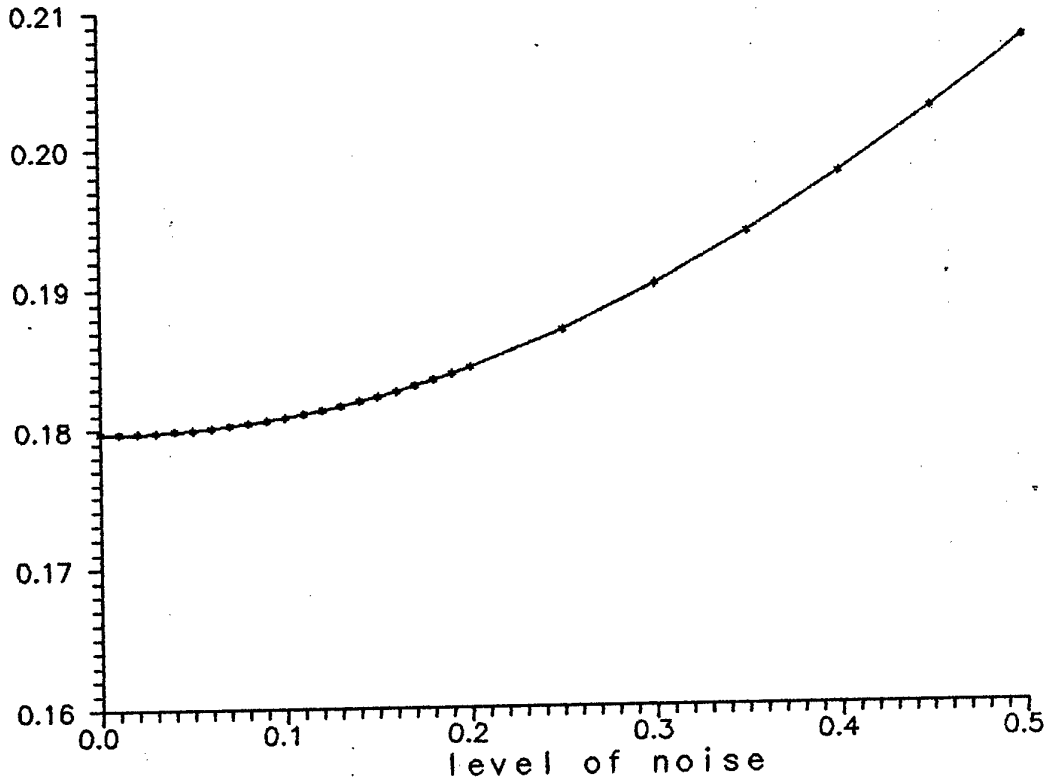

Fig 33

Table 1

Direct problem errors

Operator type	Model 5 δ_∞	Model 5 δ_2	Model 2 δ_∞	Model 2 δ_2	Model 7 δ_∞	Model 7 δ_2
A	0.0344	0.0087	0.1241	0.0803	0.3160	0.2105
B	0.0147	0.0065	0.0933	0.0540	0.0500	0.0323
C	0.0101	0.0071	0.0898	0.0534	0.0468	0.0303
D	0.0005	0.0002			0.0449	0.0244

Table 2

Inverse problem errors

Operator type	Model 5 δ_∞	Model 5 δ_2	Model 2 δ_∞	Model 2 δ_2	Model 7 δ_∞	Model 7 δ_2
A	0.26	0.21	0.328	0.226	0.407	0.327
B	0.17	0.15	0.317	0.215	0.180	0.127
C	0.16	0.14	0.316	0.215	0.161	0.118
D	0.16	0.16			0.080	0.073

Table 3

Inverse problem errors

Operator type	Model 5 Δ_∞	Model 5 Δ_2	Model 2 Δ_∞	Model 2 Δ_2	Model 7 Δ_∞	Model 7 Δ_2
A	0.25 ?	0.22	0.421	0.256	0.660	0.362
B	0.16 ?	0.14	0.339	0.225	0.170	0.089
C	0.15 ?	0.14	0.339	0.224	0.152	0.075
D	0.15 ?	0.13	0.338	0.224	0.113	0.069